Geochemistry of the dissolved loads of rivers in Southeast Coastal Region, China: Anthropogenic impact on chemical weathering and carbon sequestration

Wenjing Liu[1,2,3,4], Zhifang Xu[1,2,3,4*], Huiguo Sun[1,2,3,4], Tong Zhao[1,2,3,4], Chao Shi[1,4], Taoze Liu[5]

[1] Key Laboratory of Cenozoic Geology and Environment, Institute of Geology and Geophysics, Chinese Academy of Sciences, Beijing 100029, China

[2] CAS Center for Excellence in Life and Paleoenvironment, Beijing, 100044, China

[3] Institutions of Earth Science, Chinese Academy of Sciences, Beijing 100029, China

[4] University of Chinese Academy of Sciences, Beijing 100049, China

[5] State Key Laboratory of Environmental Geochemistry, Institute of Geochemistry, Chinese Academy of Sciences, Guiyang, Guizhou 550002, China

* Corresponding author. zfxu@mail.iggcas.ac.cn (Zhifang Xu, Tel: +86 10 82998289)

Abstract:

Southeast coastal region is the most developed and populated area in China. Meanwhile, it has been the most severe acid rain impacted region for many years. The chemical compositions and carbon isotope ratio of dissolved inorganic carbon ($\delta^{13}C_{DIC}$) of rivers were investigated to evaluate the chemical weathering and associated atmospheric CO_2 consumption rates. Mass balance calculation indicated that the dissolved loads of major rivers in the Southeast Coastal Rivers Basin (SECRB) were contributed by atmospheric (14.3%, 6.6-23.4%), anthropogenic (15.7%, 0-41.1%), silicate weathering (39.5%, 17.8-74.0%) and carbonate weathering inputs (30.6%, 3.9-62.0%). The silicate and carbonate chemical weathering rates for these river watersheds were 14.2-35.8 t km^{-2} a^{-1} and 1.8-52.1 t km^{-2} a^{-1}, respectively. The associated mean CO_2 consumption rate by silicate weathering for the whole SECRB were 191×10^3 mol km^{-2} a^{-1}. The chemical and $\delta^{13}C_{DIC}$ evidences indicated that sulfuric and nitric acid (mainly from acid deposition) was significantly involved in chemical weathering of rocks. The calculation showed an overestimation of CO_2 consumption at 0.19×10^{12} g C a^{-1} if sulfuric and nitric acid was ignored, which accounted for about 33.6% of the total CO_2 consumption by silicate weathering in the SECRB. This study quantitatively highlights that the role of acid deposition in chemical weathering, suggesting that anthropogenic impact should be seriously considered in estimation of chemical weathering and associated CO_2 consumption.

Keywords: Southeast Coastal Rivers Basin; Chemical weathering; CO_2 consumption; acid deposition;

1. Introduction

Chemical weathering of rocks is a key process that links geochemical cycling of solid earth to the atmosphere and ocean. It provides nutrients to terrestrial and marine ecosystems and regulates the level of atmospheric CO_2. As a net sink of atmospheric CO_2 on geologic timescales, estimation of silicate chemical weathering rates and the controlling factors are important issues related to long-term global climate change (e.g. Raymo and Ruddiman, 1992; Négrel et al. 1993; Berner and Caldeira, 1997; Gaillardet et al., 1999; Kump et al., 2000; Amiotte-Suchet et al., 2003; Oliva et al., 2003; Hartmann et al., 2009; Moon et al., 2014). As an important component in the Earth's Critical Zone (U.S. Nat. Res. Council Comm., 2001), river serves as an integrator of various natural and anthropogenic processes and products in a basin, and a carrier transporting the weathering products from continent to ocean. Therefore, the chemical compositions of river are widely used to evaluate chemical weathering and associated CO_2 consumption rates at catchment and/or continental scale, and examine their controlling factors (e.g., Edmond et al., 1995; Gislason et al., 1996; Galy and France-Lanord, 1999; Huh, 2003; Millot et al., 2002, 2003; Oliva et al., 2003; West et al., 2005; Moon et al., 2007; Noh et al., 2009; Shin et al., 2011; Calmels et al., 2011; Li, S., et al. 2014).

With the intensification of human activities, human perturbations to river basins have increased in frequency and magnitude (Raymond et al., 2008; Regnier et al., 2013; Li and Bush, 2015). It is important to understand how such perturbations

function on the current weathering systems and to predict how they will affect the Critical Zone of the future (Brantley and Lebedeva, 2011). In addition to CO_2, other sources of acidity (such as sulfuric, nitric and organic acids) can also produce protons. These protons react with carbonate and silicate minerals, thus enhance rock chemical weathering rate and flux compared with only considering protons deriving from CO_2 dissolution (Calmels et al., 2007; Xu and Liu, 2010). The effect of other sourced proton (especially H^+ induced by SO_2 and NO_X coming from anthropogenic activities) on chemical weathering is documented to be an important mechanism modifying atmospheric CO_2 consumption by rock weathering (Galy and France-Lanord, 1999; Semhi, et al., 2000; Spence and Telmer, 2005; Xu and Liu, 2007; Perrin et al., 2008; Gandois et al., 2011). Anthropogenic emissions of SO_2 was projected to provide 3 to 5 times greater H_2SO_4 to the continental surface than the pyrite oxidation originated H_2SO_4 (Lerman et al., 2007). Therefore, increasing acid precipitation due to intense human activities nowadays could make this mechanism more prominently.

The role of acid precipitation on the chemical weathering and CO_2 consumption has been investigated in some river catchments (Amiotte-Suchet et al., 1995; Probst et al., 2000; Vries et al., 2003; Lerman et al., 2007; Xu and Liu, 2010). It has been documented that silicate rocks were more easily disturbed by acid precipitation during their weathering and soil leaching processes, because of their low buffeting capacity (Reuss et al., 1987; Amiotte-Suchet et al., 1995). The disturbance could be intensive and cause a decrease of CO_2 consumption about 73% by weathering due to acid precipitation in the Strengbach catchment (Vosges Mountains, France), where is

dominated by crystalline rocks (Amiotte-Suchet et al., 1995). This highlights the importance of exploring anthropogenic impact on chemical weathering and CO_2 consumption under different background (e.g. lithology, climate, human activity intensity, and basin scale) for better constraining and estimation of acid precipitation effect on rock weathering. Asia, especially East Asia, is one of the world's major sulfur emissions areas. However, the effect of acid precipitation on silicate weathering and associated CO_2 consumption was not well evaluated in this area, especially lack of quantitative studies.

Acid precipitation affected about 30% of the territory of China (Fig. 1), and the seriously areas are mainly located in the east, the south and the center of China, where over 70% of cities were suffering from acid rain (Zhang et al., 2007a; State Environmental Protection Administration of China, 2009). Southeast coastal region of China is the most developed and populated area this country, dominated by Mesozoic magmatic rocks (mainly granite and volcanic rocks) in lithology. Meanwhile, the southeast coastal area has become one of the three major acid rain areas in China since the beginning of the 1990s (Larssen et al., 1999). It is seriously impacted by acid rain, with a volume-weighted mean value of pH lower than 4.5 for many years (Wang et al., 2000; Larssen and Carmichael, 2000; Zhao, 2004; Han et al., 2006; Larssen et al., 2006; Zhang et al., 2007a; Huang et al., 2008; Xu et al., 2011). Therefore, it is an ideal area for evaluating silicate weathering and the effect of acid rain. In the previous work, we have recognized and discussed the importance of sulfuric acid on the rock weathering and associated CO_2 consumption in Qiantang

river basin in this area (Liu et al., 2016). However, it is difficult to infer the anthropogenic impact on chemical weathering and CO_2 consumption in the whole southeast coastal area from the case study of the Qiantang basin, because of the variations on lithology, basin scale, runoff and anthropogenic background in a large acid deposition affected area. In this study, the chemical and carbon isotope composition of rivers in this area were first systematically investigated, in order to: (i) decipher the different sources of solutes and to quantify their contributions to the dissolved loads; (ii) calculate silicate weathering and associated CO_2 consumption rates; (iii) evaluate the effects of acid deposition on rock weathering and CO_2 consumption flux in the whole southeast coastal area.

2. Natural setting of study area

Southeast coastal region of China, where the landscape is dominated by mountainous and hilly terrain, and lacks the conditions for breeding large rivers. The rivers in this region is dominantly small and medium-sized due to the topographic limitation. Only 5 rivers in this region have length over 200 km and the drainage area over 10,000 km^2, and they are in turn from north to south: Qiantangjiang (Qiantang) and Oujiang (Ou) in Zhejiang province; Minjiang (Min) and Jiulongjiang (Jiulong) in Fujian province; Han Jiang (Han) in Guangdong province (Fig. 1). Rivers in this region generally flow eastward or southward and finally inject into the East China Sea or the South China Sea (Fig. 1), and they are collectively named as 'Southeast Coastal Rivers' (SECRs).

The Southeast Coastal Rivers Basin (SECRB) belongs to the warm and humid

122 subtropical oceanic monsoon climate. The average annual temperature and
123 precipitation are 17-21℃ and 1400-2000 mm, respectively. The precipitation mainly
124 happens during May to September, and the minimum and maximum temperature
125 often occurs in January and July. This area is one of the most developed areas in
126 China, with a population more than 190 million (mean density of ~470
127 individuals/km^2), but the population mainly concentrated in the coastal urban areas.
128 The vegetation coverage of these river basins is more than 60%, mainly subtropical
129 evergreen-deciduous broadleaf forest and mostly distributing in mountains area.
130 Cultivated land, and industries and cities are mainly located in the plain areas and
131 lower reach of these rivers.

132 Geologically, three regional-scale fault zones are distributed across the SECRB
133 region (Fig. 1). They are the sub-EW-trending Shaoxing-Jiangshan fault zone, the
134 NE-trending Zhenghe-Dapu fault zone, and the NE-trending Changle-Nanao fault
135 zone (Shu et al., 2009). These fault zones dominate the direction of the mountains
136 ridgelines and drainages, as well as the formation of the basins and bay. The Zhenghe-
137 Dapu fault zone is a boundary line of Caledonian uplift belt and Hercynian-Indosinian
138 depression zone. Mesozoic magmatic rocks are widespread in the southeast coastal
139 region with a total outcrop area at about 240,000 km^2. Over 90% of the Mesozoic
140 magmatic rocks are granitoids (granites and rhyolites) and their volcanic counterpart
141 with minor existence of basalts (Zhou et al., 2000, 2006; Bai et al., 2014). These crust-
142 derived granitic rocks are mainly formed in the Yanshanian stage, and may have been
143 related to multiple collision events between Cathaysia and Yangtze blocks and Pacific

144 plate (Zhou and Li, 2000; Xu et al., 2016). Among the major river basins, the
145 proportions of magmatic rocks outcrop are about 36% in Qiantang river basin, above
146 80% in Ou, Jiaoxi and Jin river basins, and around 60% in Min, Jiulong, Han and
147 Rong river basins (Shi, 2014). The overlying Quaternary sediment in this area is
148 composed of brown-yellow siltstones but is rarely developed. The oldest basement
149 complex is composed of metamorphic rocks of greenschist and amphibolite facies.
150 Sedimentary rocks categories into two types, one is mainly composed by red clastic
151 rocks which cover more than 40,000 km^2 in the study area; the other occurs as
152 interlayers within volcanic formations, including varicolored mudstones and
153 sandstones. They are mainly distributed on the west of Zhenghe-Dapu fault zone
154 (FJBGRM, 1985; ZJBGMR, 1989; Shu et al., 2009).

155 **3. Sampling and analytical method**

156 A total of 121 water samples were collected from mainstream and tributaries of
157 the major rivers in the SECRB from July 8th to 31 of 2010 in the high-flow period
158 (sample number and locations are shown in Fig. 1). 2-L water samples were collected
159 in the middle channel of the river from bridges or ferries, or directly from the center
160 of some shallow streams in the source area. The lower reaches sampling sites were
161 selected distant away from the estuary to avoid the influence of seawater. Temperature
162 (T), pH and electrical conductivity (EC) were measured in the field with a portable
163 EC/pH meter (YSI-6920, USA). All of the water samples for chemical analysis were
164 filtered in field through 0.22 μm Millipore membrane filter, and the first portion of the
165 filtration was discarded to wash the membrane and filter. One portion filtrate were

166 stored directly in HDPE bottles for anion analysis and another were acidified to pH <
167 2 with 6 M double sub-boiling distilled HNO_3 for cation analysis. All containers were
168 previously washed with high-purity HCl and rinsed with Milli-Q 18.2 MΩ water.

169 HCO_3^- was titrated with 0.005M HCl within 12 h after sampling. Cations (Na^+,
170 K^+, Ca^{2+} and Mg^{2+}) were determined using Inductively Coupled Plasma Atomic
171 Emission Spectrometer (ICP-AES) (IRIS Intrepid II XSP, USA). Anions (Cl^-, F^-,
172 NO_3^- and SO_4^{2-}) were analyzed by ionic chromatography (IC) (Dionex Corporation,
173 USA). Dissolved silica was determined by spectrophotometry using the molybdate
174 blue method. Reagent and procedural blanks were measured in parallel to the sample
175 treatment, and calibration curve was evaluated by quality control standards before,
176 during and after the analyses of each batch of samples. Measurement reproducibility
177 was determined by duplicated sample and standards, which showed ±3% precision for
178 the cations and ±5% for the anions.

179 River water samples for carbon isotopic ratio ($\delta^{13}C$) of dissolved inorganic
180 carbon (DIC) measurements were collected in 150 ml glass bottles with air-tight caps
181 and preserved with $HgCl_2$ to prevent biological activity. The samples were kept
182 refrigerated until analysis. For the $\delta^{13}C$ measurements, the filtered samples were
183 injected into glass bottles with phosphoric acid. The CO_2 was then extracted and
184 cryogenically purified using a high vacuum line. $\delta^{13}C$ isotopic ratios were analyzed on
185 Finnigen MAT-252 stable isotope mass spectrometer at the State Key Laboratory of
186 Environmental Geochemistry, Chinese Academy of Sciences. The results are
187 expressed with reference to VPDB, as follows:

188 $$\delta^{13}C = [((^{13}C/^{12}C)_{sample} / (^{13}C/^{12}C)_{standard}) - 1] \times 1000 \quad (1)$$

189 The $\delta^{13}C$ measurement has an overall precision of 0.1‰. A number of duplicate
190 samples were measured and the results show that the differences were less than the
191 range of measurement accuracy.

192 **4. Results**

193 The major parameter and ion concentrations of samples are given in Table 1. The
194 pH values of water samples ranged from 6.50 to 8.24, with an average of 7.23. Total
195 dissolved solids (TDS) of water samples varied from 35.3 to 205 mg l^{-1}, with an
196 average of 75.2 mg l^{-1}. Compared with the major rivers in China, the average TDS
197 was significantly lower than the Changjiang (224 mg l^{-1}, Chetelat et al., 2008) , the
198 Huanghe (557 mg l^{-1}, Fan et al., 2014) and the Zhujiang (190 mg l^{-1}, Zhang et al.,
199 2007b). However, the average TDS was comparable to the rivers draining silicate rock
200 dominated areas, e.g. the upper Ganjiang in Ganzhou, south China (63 mg l^{-1}, Ji and
201 Jiang, 2012), the Amur in north China (70 mg l^{-1}, Moon et al., 2009), the Xishui in
202 Hubei, central China (101 mg l^{-1}, Wu et al., 2013), and north Han river in South Korea
203 (75.5 mg l^{-1}, Ryu et al., 2008). Among the major rivers in the SECRB, the Qiantang
204 had the highest TDS value (averaging at 121 mg l^{-1}), and the Ou had the lowest TDS
205 value (averaging at 48.8 mg l^{-1}).

206 Major ion compositions are shown in the cation and anion ternary diagrams (Fig.
207 2a and b). In comparison with rivers (e.g. the Wujiang and Xijiang) draining
208 carbonate rocks dominated area (Han and Liu, 2004; Xu and Liu, 2010), these rivers
209 in the SECRB have distinctly higher proportions of Na^+, K^+, and dissolved SiO_2. As

shown in the Fig. 2, most samples have high Na^+ and K^+ proportions, with an average more than 50% (in μmol l^{-1}) of the total cations, except for samples from the Qiantang. The concentrations of Na^+ and K^+ range from 43.5 to 555 μmol l^{-1} and 42.9 to 233 μmol l^{-1}, with average values of 152 and 98 μmol l^{-1}, respectively. The concentrations of dissolved SiO_2 range from 98.5 to 370 μmol l^{-1}, with an average of 212 μmol l^{-1}. Ca^{2+} and Mg^{2+} account for about 38% and 11.6% of the total cation concentrations. HCO_3^- is the dominant anion with concentrations ranging from 139 to 1822 μmol l^{-1}. On average, it comprises 60.6% (36-84.6%) of total anions on a molar basis, followed by SO_4^{2-} (14.6%), Cl^- (13.1%) and NO_3^- (11.8%). The major ionic compositions indicate that water chemistry of these rivers in the SECRB is controlled by silicate weathering. Meanwhile, it is also influenced by carbonate weathering, especially in the Qiantang river system.

The $\delta^{13}C$ of dissolved inorganic carbon in the rivers of the SECRB are given in Table 1. The $\delta^{13}C$ of the water samples show a wide range, from -11.0‰ to -24.3‰ (average -19.4‰), and with majority falling between -15 and -23‰. The values are similar to rivers draining Deccan Traps (Das et al., 2005).

5. Discussion

The dissolved solids in river water are commonly from atmospheric and anthropogenic inputs and weathering of rocks within the drainage basin. It is necessary to quantify the contribution of different sources to the dissolved loads before deriving chemical weathering rates and associated CO_2 consumption.

5.1 Atmospheric and anthropogenic inputs

To evaluate atmospheric inputs to river waters, chloride is the most common used reference. Generally, water samples that have the lowest Cl^- concentrations are employed to correct the proportion of atmospheric inputs in a river system (Négrel et al., 1993; Gaillardet et al., 1997; Viers et al., 2001; Xu and Liu, 2007). In pristine areas, the concentration of Cl^- in river water is assumed to be entirely derived from the atmosphere, provided that the contribution of evaporites is negligible (e.g. Stallard and Edmond, 1981; Négrel et al., 1993). In the SECRB, the lowest Cl^- concentration was mainly found in the headwater of each river. According to the geologic setting, no salt-bearing rocks was found in these headwater area (FJBGRM, 1985; ZJBGMR, 1989). In addition, these areas are mainly mountainous and sparsely populated. Therefore, we assumed that the lowest Cl^- concentration of samples from the headwater of each major river came entirely from atmosphere.

The proportion of atmosphere-derived ions in the river waters can then be calculated by using the element/Cl ratios of the rain. Chemical compositions of rain in the studied area have been reported at different sites, including Hangzhou, Jinhua, Nanping, Fuzhou and Xiamen (Zhao, 2004; Zhang et al., 2007a; Huang et al., 2008; Cheng et al., 2011; Xu et al., 2011) (Fig. 1). The volume-weighted mean concentration of ions and Cl-normalized molar ratios are compiled in Table 2. According to this procedure, 6.6-23.4% (averaging 14.3%) of total dissolved cations in the major rivers of the SECRB originated from rain. Among the anions, SO_4^{2-} and NO_3^- in the rivers are mainly from the atmospheric input, averaging at 74.7% for SO_4^{2-} and 68.6% for NO_3^-, respectively.

As the most developed and populated areas in China, the chemistry of rivers in the SECRB could be significantly impacted by anthropogenic inputs. Cl^-, NO_3^- and SO_4^{2-} are commonly associated with anthropogenic sources and have been used as tracers of anthropogenic inputs in watershed. High concentrations of Cl^-, NO_3^- and SO_4^{2-} can be found at the lower reaches of rivers in the SECRB, and an obvious increase after flowing through plain areas and cities. This tendency indicates that river water chemistry is affected by anthropogenic inputs while passing through the catchments. After correcting for the atmospheric contribution to river waters, the following assumption is needed to quantitatively estimate the contributions of anthropogenic inputs. That is, Cl^- originates from only atmospheric and anthropogenic inputs, the excess of atmospheric Cl^- is regarded to present anthropogenic inputs and balanced by Na^+.

5.2 Chemical weathering inputs

Water samples were displayed on a plot of Na-normalized molar ratios (Fig. 3). The values of the world's large rivers (Gaillardet et al. 1999) are also shown in the figure. A best correlations between elemental ratios were observed for Ca^{2+}/Na^+ vs. Mg^{2+}/Na^+ (R^2 = 0.95, n = 120) and Ca^{2+}/Na^+ vs. HCO_3^-/Na^+ (R^2 = 0.98, n = 120). The samples cluster on a mixing line mainly between silicate and carbonate end-members, closer to the silicate end-member, and with little evaporite contribution. This corresponds with the distribution of rock types in the SECRB. In addition, all water samples have equivalent ratios of $(Na^+ + K^+)/Cl^-$ larger than one, indicating silicate weathering as the source of Na^+ and K^+ rather than chloride evaporites dissolution.

276 The geochemical characteristics of the silicate and carbonate end-members can
277 be deduced from the correlations between elemental ratios and referred to literature
278 data for catchments with well-constrained lithology. After correction for atmospheric
279 inputs, the Ca^{2+}/Na^{+}, Mg^{2+}/Na^{+} and HCO_3^{-}/Na^{+} of the river samples ranged from 0.31
280 to 30, 0.16 to 6.7, and 1.1 to 64.2, respectively. According to the geological setting
281 (Fig. 1), there are some small rivers draining purely silicate areas in the SECRs
282 drainage basins. Based on the elemental ratios of these rivers, we assigned the silicate
283 end-member for this study as Ca^{2+}/Na^{+}=0.41±0.10, Mg^{2+}/Na^{+}=0.20±0.03 and HCO_3^{-}
284 $/Na^{+}$=1.7±0.6. The ratio of $(Ca^{2+}+Mg^{2+})/Na^{+}$ for silicate end-member was 0.61, which
285 is close to the silicate end-member of world rivers ($(Ca^{2+}+Mg^{2+})/Na^{+}$=0.59±0.17,
286 Gaillardet et al., 1999). Moreover, several previous researches have documented the
287 chemical composition of rivers, such as the Amur and the Songhuajiang in North
288 China, the Xishui in the lower reaches of the Changjiang, and major rivers in South
289 Korea (Moon et al., 2009; Liu et al., 2013; Wu et al., 2013; Ryu et al., 2008; Shin et
290 al., 2011). These river basins has similar lithological setting with the study area, we
291 could further validate the composition of silicate end-member with their results.
292 Ca^{2+}/Na^{+} and Mg^{2+}/Na^{+} ratios of silicate end-member were reported for the Amur
293 (0.36 and 0.22), the Songhuajiang (0.44±0.23 and 0.16), the Xishui (0.6±0.4 and
294 0.32±0.18), the Han (0.55 and 0.21) and six major rivers in South Korea (0.48 and
295 0.20) in the studies above, well bracketing our estimation for silicate end-member.
296 Whereas, some samples show high concentrations of Ca^{2+}, Mg^{2+} and HCO_3^{-},
297 indicating the contribution of carbonate weathering. The samples collected in the

upper reaches (Sample 12 and 13) in the Qiantang fall close to the carbonate end-member documented for world large rivers (Gaillardet et al., 1999). In the present study, Ca^{2+}/Na^{+} ratio of 0.41±0.10 and Mg^{2+}/Na^{+} ratio of 0.20±0.03 for silicate end-member are used to calculate the contribution of Ca^{2+} and Mg^{2+} from silicate weathering. Finally, residual Ca^{2+} and Mg^{2+} are apportioned to carbonate weathering.

5.3 Chemical weathering rate in the SECRBs

Based on the above assumption, a forward model is employed to quantify the relative contribution of the different sources to the rivers of the SECRB in this study. (e.g. Galy and France-Lanord, 1999; Moon et al., 2007; Xu and Liu, 2007; 2010; Liu et al., 2013). The calculated contributions of different reservoir to the total cationic loads for large rivers and their major tributaries in the SECRB are presented in Fig. 4. On average, the dissolved cationic loads of the rivers in the study area originate dominantly from silicate weathering, which accounts for 39.5% (17.8-74.0%) of the total cationic loads in molar unit. Carbonate weathering and anthropogenic inputs account for 30.6% (3.9-62.0%) and 15.7% (0-41.1%), respectively. Contributions from silicate weathering are high in the Ou (55.6%), the Huotong (54.5%), the Ao (48.3%) and the Min (48.3%) river catchments, which dominated by granitic and volcanic bedrocks. In contrast, high contribution from carbonate weathering is observed in the Qiantang (54.0%), the Jin (52.2%) and the Jiulong (44.8%) river catchments. The results manifest the lithology control on river solutes of drainage basin.

The chemical weathering rate of rocks is estimated by the mass budget, basin

area and annual discharge (data from the Annual Hydrological Report P. R. China, 2010, Table 3), expressed in ton km^{-2} a^{-1}. The silicate weathering rate (SWR) is calculated using major cationic concentrations from silicate weathering and assuming that all dissolved SiO_2 is derived from silicate weathering (Xu and Liu, 2010), as the equation below:

$$SWR = ([Na]_{sil} + [K]_{sil} + [Ca]_{sil} + [Mg]_{sil} + [SiO_2]_{riv}) \times discharge/area \quad (2)$$

The assumption about Si could lead to overestimation of the silicate weathering rate, as part of silica may come from dissolution of biogenic sources rather than the weathering of silicate minerals (Millot et al., 2003; Shin et al., 2011). Thus, the cationic silicate weathering rates (Cat_{sil}) were also calculated.

The carbonate weathering rate (CWR) is calculated based on the sum of Ca^{2+}, Mg^{2+} and HCO_3^- from carbonate weathering, with half of the HCO_3^- coming from carbonate weathering being derived from the atmosphere CO_2, as the equation below:

$$CWR = ([Ca]_{carb} + [Mg]_{carb} + 1/2[HCO_3]_{carb}) \times discharge/area \quad (3)$$

The chemical weathering rate and flux are calculated for major rivers and their main tributaries in the SECRB, and the results are shown in Table 3. Silicate and carbonate weathering fluxes of these rivers (SWF and CWF) range from 0.02×10^6 t a^{-1} to 1.80×10^6 t a^{-1}, and from 0.004×10^6 t a^{-1} to 1.74×10^6 t a^{-1}, respectively. Among the rivers, the Min has the highest silicate weathering flux, and the Qiantang has the highest carbonate weathering flux. On the whole SECRB scale, 3.95×10^6 t a^{-1} and 4.09×10^6 t a^{-1} of dissolved solids originating from silicate and carbonate weathering, respectively, are transported into the East and South China Sea by rivers in this

region. Compared with the largest three river basins (the Changjiang, the Huanghe and the Xijiang) in China, the flux of silicate weathering calculated for the SECRB is lower than the Changjiang (9.5×10^6 t a^{-1}, Gaillardet et al. 1999), but higher than the Huanghe (1.52×10^6 t a^{-1}, Fan et al., 2014) and the Xijiang (2.62×10^6 t a^{-1}, Xu and Liu, 2010).

The silicate and carbonate chemical weathering rates for these river watersheds were 14.2-35.8 t km^{-2} a^{-1} and 1.8-52.1 t km^{-2} a^{-1}, respectively. The total rock weathering rate (TWR) for the whole SECRB is 48.1 ton km^{-2} a^{-1}, higher than the world average (24 ton km^{-2} a^{-1}, Gaillardet et al., 1999). The cationic silicate weathering rates (Cat_{sil}) ranges from 4.7 to 12.0 ton km^{-2} a^{-1} for the river watersheds in the SECRB, averaging at 7.8 ton km^{-2} a^{-1}. Furthermore, a good linear correlation (R^2 = 0.77, n = 28) is observed between the Cat_{sil} and runoff (Fig. 5), indicating silicate weathering rates is controlled by the runoff as documented in previous researches (e.g., Bluth and Kump, 1994; Gaillardet et al., 1999; Millot et al., 2002; Oliva et al., 2003; Wu et al., 2013; Pepin et al., 2013).

5.4 CO_2 consumption and the role of sulfuric acid

To calculate atmospheric CO_2 consumption by silicate weathering (CSW) and by carbonate weathering (CCW), a charge-balanced state between rock chemical weathering-derived alkalinity and cations was assumed (Roy et al., 1999).

$$[CO_2]_{CSW} = [HCO_3]_{CSW} = [Na]_{sil} + [K]_{sil} + 2[Ca]_{sil} + 2[Mg]_{sil} \quad (4)$$

$$[CO_2]_{CCW} = [HCO_3]_{CCW} = [Ca]_{carb} + [Mg]_{carb} \quad (5)$$

The calculated CO_2 consumption rates by chemical weathering for the studied

rivers in SECRB are shown in Table 3. CO_2 consumption rates by carbonate and silicate weathering are from 17.9 to 530×10^3 mol km^{-2} a^{-1} (averaging at 206×10^3 mol km^{-2} a^{-1}) and from 167 to 460×10^3 mol km^{-2} a^{-1} (averaging at 281×10^3 mol km^{-2} a^{-1}) for major river catchments in the SECRB. The CO_2 consumption rates by silicate weathering in the SECRB are higher than that of major rivers in the world and China, such as the Amazon (174×10^3 mol km^{-2} a^{-1}, Mortatti and Probst, 2003), the Mississippi and the Mackenzie (66.8 and 34.1×10^3 mol km^{-2} a^{-1}, Gaillardet et al., 1999), the Changjiang (112×10^3 mol km^{-2} a^{-1}, Chetelat et al., 2008), the Huanghe (35×10^3 mol km^{-2} a^{-1}, Fan et al., 2014), the Xijiang (154×10^3 mol km^{-2} a^{-1}, Xu and Liu, 2010), the Longchuanjiang (173×10^3 mol km^{-2} a^{-1}, Li et al., 2011) and the Mekong (191×10^3 mol km^{-2} a^{-1}, Li et al., 2014) and three large rivers in eastern Tibet (103-121×10^3 mol km^{-2} a^{-1}, Noh et al., 2009), the Hanjiang in central China (120×10^3 mol km^{-2} a^{-1}, Li et al., 2009) and the Sonhuajiang in north China (66.6×10^3 mol km^{-2} a^{-1}, Liu et al., 2013). The high CO_2 consumption rates by silicate weathering in the SECRB could be attributed to extensive distribution of silicate rocks, high runoff, humid and hot climatic conditions. The regional fluxes of CO_2 consumption by silicate and carbonate weathering is about 47.9×10^9 mol a^{-1} (0.57×10^{12} g C a^{-1}) and 41.9×10^9 mol a^{-1} (0.50×10^{12} g C a^{-1}) in the SECRB.

However, in addition to CO_2, the anthropogenic sourced proton (e.g. H_2SO_4 and HNO_3) is well documented as significant proton providers in rock weathering process (Galy and France-Lanord, 1999; Karim and Veizer, 2000; Yoshimura et al., 2001; Han and Liu, 2004; Spence and Telmer, 2005; Lerman and Wu, 2006; Xu and Liu 2007;

386 2010; Perrin et al., 2008; Gandois et al., 2011). Sulfuric acid can be generated by
387 natural oxidation of pyrite and anthropogenic emissions of SO_2 from coal combustion
388 and subsequently dissolve carbonate and silicate minerals. The riverine nitrate in
389 watersheds can be derived from atmospheric deposition, synthetic fertilizers,
390 microbial nitrification, sewage and manure, etc. (e.g. Kendall 1998). Although it is
391 difficult to determine the origin of nitrate in river waters, we can simply assume that
392 nitrate from acid deposition is one of the providers of protons. The consumption of
393 CO_2 by rock weathering would be overestimated if H_2SO_4 and HNO_3 induced rock
394 weathering is ignored (Spence and Telmer, 2005; Xu and Liu, 2010; Shin et al., 2011;
395 Gandois et al., 2011). Thus, the role of the anthropogenic sourced protons on the
396 chemical weathering is crucial for an accurate estimation of CO_2 consumption by rock
397 weathering.

398 Rapid economic growth and increased energy command have result in severe air
399 pollution problems in China, indicated by the high levels of mineral acids
400 (predominately sulfuric) observed in precipitation (Lassen and Carmichael, 2000; Pan
401 et al., 2013; Liu et al., 2016). The national SO_2 emissions in 2010 reached to 30.8
402 Tg/year (Lu et al., 2011). Previous study documented that fossil fuel combustion
403 accounts for the dominant sulfur deposition (~77%) in China (Liu et al., 2016). The
404 wet deposition rate of nitrogen peaked over the central and south China, with mean
405 value of 20.2, 18.2 and 25.8 kg N ha^{-1} yr^{-1} in Zhejiang, Fujian and Guangdong
406 province, respectively (Lu and Tian, 2007). Current sulfur and nitrogen depositions in
407 the Southeast coastal region are still among the highest in China (Fang et al., 2013;

Cui et al., 2014; Liu et al., 2016).

The involvement of protons originating from H_2SO_4 and HNO_3 in the river waters can be verified by the stoichiometry between cations and anions, shown in Fig. 6. In the rivers of the SECRB, the sum cations released by silicate and carbonate weathering were not balanced by HCO_3^- only (Fig. 6a), but were almost balanced by the sum of HCO_3^- and SO_4^{2-} and NO_3^- (Fig. 6b). This implies that H_2CO_3 and H_2SO_4 and HNO_3 are the potential erosion agents in chemical weathering in the SECRB. The $\delta^{13}C$ values of the water samples show a wide range, from -11.0‰ to -24.3‰, with an average of -19.4‰. The $\delta^{13}C$ from soil is governed by the relative contribution from C_3 and C_4 plant (Das et al., 2005). The studied areas have subtropical temperatures and humidity, and thus C_3 processes are dominant. The $\delta^{13}C$ of soil CO_2 is derived primarily from $\delta^{13}C$ of organic material which typically has a value of -24 to -34‰, with an average of -28‰ (Faure, 1986). According to previous studies, the average value for C_3 trees and shrubs are from -24.4 to -30.5‰, and most of them are lower than -28‰ in south China (Chen et al., 2005; Xiang, 2006; Dou et al., 2013). After accounting for the isotopic effect from diffusion of CO_2 from soil, the resulting $\delta^{13}C$ (from the terrestrial C_3 plant process) should be ~ -25‰ (Cerling et al., 1991). This mean DIC derived from silicate weathering by carbonic acid (100% from soil CO_2) would yield a $\delta^{13}C$ value of -25‰. Carbonate rocks are generally derived from marine system and, typically, have $\delta^{13}C$ value close to zero (Das et al., 2005). Thus, the theoretical $\delta^{13}C$ value of DIC derived from carbonate weathering by carbonic acid (50% from soil CO_2 and 50% from carbonate rocks) is -12.5‰. DIC derived from

carbonate weathering by sulfuric acid are all from carbonate rocks, thus the $\delta^{13}C$ of the DIC would be 0‰. Based on these conclusions, sources of riverine DIC from different end-members in the SECRB were plotted in Fig. 7. Most water samples drift away from the three endmember mixing area (carbonate and silicate weathering by carbonic acid and carbonate weathering by sulfuric acid) and towards the silicate weathering by sulfuric acid area, clearly illustrating the effect of the anthropogenic sourced protons on silicate weathering in the SECRB.

Considering the H_2SO_4 and HNO_3 effect on chemical weathering, CO_2 consumption by silicate weathering can be determined from the equation below (Moon et al., 2007; Ryu et al., 2008; Shin et al., 2011):

$$[CO_2]_{SSW} = [Na]_{sil} + [K]_{sil} + 2[Ca]_{sil} + 2[Mg]_{sil} - \gamma\times[2SO_4+NO_3]_{atmos} \quad (6)$$

Where γ is calculated by $cation_{sil}/(cation_{sil} + cation_{carb})$.

Based on the calculation in section 5.1, SO_4^{2-} and NO_3^- in river waters were mainly derived from atmospheric input. Assuming SO_4^{2-} and NO_3^- in river waters derived from atmospheric input (after correction for sea-salt contribution) are all from acid precipitation, CO_2 consumption rates by silicate weathering (SSW) are estimated between 55×10^3 mol km^{-2} a^{-1} and 286×10^3 mol km^{-2} a^{-1} for major river watersheds in the SECRB. For the whole SECRB, the actual CO_2 consumption rates by silicate is 191×10^3 mol km^{-2} a^{-1} when the effect of H_2SO_4 is considered. The flux of CO_2 consumption is overestimated by 16.1×10^9 mol a^{-1} (0.19×10^{12} g C a^{-1}) due to the involvement of sulfuric acid from acid precipitation, accounting for approximately 33.6% of total CO_2 consumption flux by silicate weathering in the SECRB. It

highlights the fact that the drawdown of atmospheric CO_2 by silicate weathering can be significantly overestimated if acid deposition is ignored in short- and long-term perspectives. The result is important as it quantitatively shows that anthropogenic activities can significantly affect rock weathering and associated atmospheric CO_2 consumption. The quantification of this effect needs to be well evaluated in Asian and global scale within the current and future human activity background.

6. Conclusions

River waters in the Southeast coastal region of China are characterized by high proportions of Na^+, K^+ and dissolved SiO_2, indicating water chemistry of the rivers in the SECRB is mainly controlled by silicate weathering. The dissolved cationic loads of the rivers in the study area originate dominantly from silicate weathering, which accounts for 39.5% (17.8-74.0%) of the total cationic loads. Carbonate weathering, atmospheric and anthropogenic inputs account for 30.6%, 14.3% and 15.7%, respectively. Meanwhile, more than 70% of SO_4^{2-} in the rivers derived from atmospheric input. The chemical weathering rate of silicates and carbonates for the whole SECRB are estimated to be approximately 23.7 and 24.5 ton km^{-2} a^{-1}. About 8.04×10^6 t a^{-1} of dissolved solids originating from rock weathering are transported into the East and South China Sea by these rivers. With the assumption that all the protons involved in the weathering reaction are provided by carbonic acid, the CO_2 consumption rates by silicate and carbonate weathering are 287 and 251×10^3 mol km^{-2} a^{-1}, respectively. However, both water chemistry and carbon isotope data provide evidence that sulfuric and nitric acid from acid precipitation serves as significant

agents during chemical weathering. Considering the effect of sulfuric and nitric acid, the CO_2 consumption rate by silicate weathering for the SECRB are 191×10^3 mol km^{-2} a^{-1}. Therefore, the CO_2 consumption flux would be overestimated by 16.1×10^9 mol a^{-1} (0.19×10^{12} g C a^{-1}) in the SECRB if the effect of sulfuric and nitric acid is ignored. This work illustrates that anthropogenic disturbance by acid precipitation has profound impact on CO_2 sequestration by rock weathering.

Acknowledgements. This work was financially supported by Natural Science Foundation of China (Grant No. 41673020, 91747202, 41772380 and 41730857) and the "Strategic Priority Research Program" of the Chinese Academy of Sciences (Grant No. XDB15010405).

References:

Amiotte-Suchet, P., Probst, A. Probst, J.-L., Influence of acid rain on CO_2 consumption by rock weathering: local and global scales. Water Air Soil Pollut. 85, 1563-1568, 1995.

Amiotte-Suchet, P., Probst, J.-L. Ludwig, W., Worldwide distribution of continental rock lithology: implications for the atmospheric/soil CO_2 uptake by continental weathering and alkalinity river transport to the oceans. Global Biogeochem. Cycles 17, 1038-1052, 2003.

Bai, H., Song, L.S., Xia, W.P., Prospect analysis of hot dry rock (HDR) in Eastern part of Jiangxi province, Coal Geol. China 26, 41-44. (In Chinese), 2014.

Berner, R.A., Caldeira, K., The need for mass balance and feedback in the geochemical carbon cycle. Geology 25, 955-956, 1997.

Bluth, G.J.S., Kump, L.R., Lithological and climatological controls of river chemistry. Geochim. Cosmochim. Acta 58, 2341-2359, 1994.

Brantley, S.L., Lebedeva, M., Learning to read the chemistry of regolith to understand the Critical Zone. Annual Review of Earth and Planetary Sciences, 39: 387-416, 2011.

Calmels, D., Gaillardet, J., Brenot, A., France-Lanord, C., Sustained sulfide oxidation by physical erosion processes in the Mackenzie River basin: climatic perspectives. Geology 35, 1003-1006, 2007.

Calmels, D., Galy, A., Hovius, N., Bickle, M., West, A.J., Chen, M.-C., Chapman, H., Contribution of deep groundwater to the weathering budget in a rapidly eroding mountain belt, Taiwan. Earth Planet. Sci. Lett. 303, 48-58, 2011.

Cerling, T.E., Solomon, D.K., Quade, J., Bownman, J.R., On the isotopic composition of soil CO_2. Geochim. Cosmochim. Acta 55, 3403–3405, 1991.

Chen, Q., Shen, C., Sun, Y., Peng, S., Yi, W., Li Z., Jiang, M., Spatial and temporal distribution of carbon isotopes in soil organic matter at the Dinghushan Biosphere Reserve, South China. Plant and Soil, 273: 115–128, 2005.

Cheng, Y., Liu, Y., Huo, M., Sun, Q., Wang, H., Chen, Z., Bai, Y., Chemical characteristics of precipitation at Nanping Mangdang Mountain in eastern China during spring. J. Environ. Sci. 23, 1350-1358, 2011.

Chetelat, B., Liu, C., Zhao, Z., Wang, Q., Li, S., Li, J., Wang, B., Geochemistry of the dissolved load of the Changjiang Basin rivers: anthropogenic impacts and chemical weathering. Geochim. Cosmochim. Acta 72, 4254-4277, 2008.

518 Cui, J., Zhou, J., Peng, Y., He, Y., Yang, H., Mao, J., Atmospheric wet deposition of
519 nitrogen and sulfur to a typical red soil agroecosystem in Southeast China
520 during the ten-year monsoon seasons (2003-2012). Atmos. Environ. 82, 121-
521 129, 2014.
522 Das, A., Krishnaswami, S., Sarin, M.M., Pande, K., Chemical weathering in the
523 Krishna Basin and Western Ghats of the Deccan Traps, India: Rates of basalt
524 weathering and their controls. Geochim. Cosmochim. Acta 69(8), 2067-2084,
525 2005.
526 Dou, X., Deng, Q., Li, M., Wang, W., Zhang, Q., Cheng, X., Reforestation of Pinus
527 massoniana alters soil organic carbon and nitrogen dynamics in eroded soil in
528 south China. Ecological Engineering 52, 154-160, 2013.
529 Edmond, J.M., Palmer, M.R., Measures, C.I., Grant, B., Stallard, R.F., The fluvial
530 geochemistry and denudation rate of the Guayana Shield in Venezuela,
531 Colombia, and Brazil. Geochim. Cosmochim. Acta 59, 3301-3325, 1995.
532 Fan, B.L, Zhao, Z.Q., Tao, F.X., Liu, B.J., Tao, Z.H., Gao, S., He, M.Y.,
533 Characteristics of carbonate, evaporite and silicate weathering in Huanghe River
534 basin: A comparison among the upstream, midstream and downstream. J. Asian
535 Earth Sci. 96, 17-26, 2014.
536 Fang, Y., Wang, X., Zhu, F., Wu, Z., Li, J., Zhong, L., Chen, D., Yoh, M., Three-
537 decade changes in chemical composition of precipitation in Guangzhou city,
538 southern China: has precipitation recovered from acidification following
539 sulphur dioxide emission control? Tellus B 65, 1-15, 2013.

Faure, G., Principles of Isotope Geology. Wiley, Toronto, pp. 492-493, 1986.

FJBGMR: Fujian Bureau of Geology and Mineral Resources, Regional Geology of Fujian Province. Geol. Publ. House, Beijing, p. 671 (in Chinese with English abstract), 1985.

Gaillardet, J., Dupré, B., Allègre, C.J., Négrel, P., Chemical and physical denudation in the Amazon River basin. Chem. Geol. 142, 141-173, 1997.

Gaillardet, J., Dupré, B., Louvat, P., Allegre, C.J., Global silicate weathering and CO2 consumption rates deduced from the chemistry of large rivers. Chem. Geol. 159, 3-30, 1999.

Galy, A., France-Lanord, C., Weathering processes in the Ganges-Brahmaputra basin and the riverine alkalinity budget. Chem. Geol. 159, 31-60, 1999.

Gandois, L., Perrin, A.-S., Probst, A., Impact of nitrogenous fertilizer-induced proton release on cultivated soils with contrasting carbonate contents: A column experiment. Geochim. Cosmochim. Acta 75, 1185-1198, 2011.

Gislason, S.R., Arnorsson, S., Armannsson, H., Chemical weathering of basalt in southwest Iceland: effects of runoff, age of rocks and vegetative/glacial cover. Am. J. Sci. 296, 837-907, 1996.

Han, G., Liu, C.Q., Water geochemistry controlled by carbonate dissolution: a study of the river waters draining karst-dominated terrain, Guizhou Province, China. Chem. Geol. 204, 1-21, 2004.

Han, Z.W., Ueda, H., Sakurai, T., Model study on acidifying wet deposition in East Asia during wintertime. Atmos. Environ. 40, 2360-2373, 2006.

562 Hartmann, J., Jansen, N., Dürr, H.H., Kempe, S., Köhler, P., Global CO_2 consumption
563 by chemical weathering: what is the contribution of highly active weathering
564 regions? Global Planet. Change 69, 185-194, 2009.
565 Huang, K., Zhuang, G., Xu, C., Wang Y., Tang A., The chemistry of the severe acidic
566 precipitation in Shanghai, China. Atmos. Res. 89, 149-160, 2008.
567 Huh, Y.S., Chemical weathering and climate - a global experiment: a review. Geosci.
568 J. 7, 277-288, 2003.
569 Hydrological data of river basins in Zhejiang, Fujian province and Taiwan region,
570 Annual Hydrological Report P. R. China, 2010, Vol (7) (in Chinese)
571 Ji, H., Jiang, Y., Carbon flux and C, S isotopic characteristics of river waters from a
572 karstic and a granitic terrain in the Yangtze River system. J. Asian Earth Sci. 57,
573 38-53, 2012.
574 Karim, A., Veizer, H.E., Weathering processes in the Indus River Basin: implication
575 from riverine carbon, sulphur, oxygen and strontium isotopes. Chem. Geol. 170,
576 153-177, 2000.
577 Kendall, C., Tracing nitrogen sources and cycling in catchments. In: Kendall, C., &
578 McDonnell, J.J., (Eds) Isotope Tracers in Catchment Hydrology. Elsevier,
579 Amsterdam, 1998.
580 Kump, L.R., Brantley, S.L., Arthur, M.A., Chemical weathering, atmospheric CO_2 and
581 climate. Ann. Rev. Earth Planet. Sci. 28, 611-667, 2000.
582 Larssen, T., Carmichael, G.R., Acid rain and acidification in China: the importance of
583 base cation deposition. Environ. Poll. 110, 89-102, 2000.

584 Larssen, T., Lydersen, E., Tang, D., He, Y., Gao, J., Liu, H., Duan, L., Seip, H.M.,
585 Acid rain in China. Environ. Sci. Technol. 40, 418-425, 2006.
586 Lerman, A., Wu, L., CO_2 and sulfuric acid controls of weathering and river water
587 composition. J. Geochem. Explor. 88, 427-430, 2006.
588 Lerman, A., Wu, L., Mackenzie, F.T., CO_2 and H_2SO_4 consumption in weathering and
589 material transport to the ocean, and their role in the global carbon balance. Mar.
590 Chem. 106, 326-350, 2007.
591 Li, S., Bush, R.T., Changing fluxes of carbon and other solutes from the Mekong
592 River. Sci. Rep. 5, 16005, 2015.
593 Li, S.Y., Lu, X.X., Bush, R.T., Chemical weathering and CO_2 consumption in the
594 Lower Mekong River. Sci. Total Environ. 472, 162-177, 2014.
595 Li, S.Y., Lu, X.X., He, M., Zhou, Y., Bei, R., Li, L., Zieglera, A.D., Major element
596 chemistry in the Upper Yangtze River: a case study of the Longchuanjiang
597 River. Geomorphology129, 29-42, 2011.
598 Li, S.Y., Xu, Z.F., Wang, H., Wang, J.H., Zhang, Q.F., Geochemistry of the upper Han
599 River basin, China. 3: anthropogenic inputs and chemical weathering to the
600 dissolved load. Chem. Geol. 264, 89-95, 2009.
601 Liu, B., Liu, C.-Q., Zhang, G., Zhao, Z.-Q., Li, S.-L., Hu, J., Ding, H., Lang, Y.-C.,
602 Li., X.-D., Chemical weathering under mid- to cool temperate and monsoon-
603 controlled climate: A study on water geochemistry of the Songhuajiang River
604 system, northeast China. Appl. Geochem. 31, 265-278, 2013.
605 Liu, L., Zhang, X., Wang, S., Zhang, W., Lu, X., Bulk sulfur (S) deposition in China.

606 Atmos. Environ., 135, 41-49, 2016.
607 Liu, W., Shi, C., Xu, Z., Zhao, T., Jiang, H., Liang, C., Zhang, X., Zhou, Li., Yu, C.,
608 Water geochemistry of the Qiantangjiang River, East China: Chemical
609 weathering and CO_2 consumption in a basin affected by severe acid deposition.
610 J.Asian Earth Sci., 127, 246-256, 2016.
611 Lu, C., Tian, H., Spatial and temporal patterns of nitrogen deposition in China:
612 Synthesis of observational data. J. Geophys. Res. 112, D22S05, 2007.
613 Lu, Z., Zhang, Q., Streets, D.G., Sulfur dioxide and primary carbonaceous aerosol
614 emissions in China and India, 1996e2010. Atmos. Chem. Phys. 11, 9839-9864,
615 2011.
616 Millot, R., Gaillardet, J., Dupré, B., Allègre, C.J., Northern latitude chemical
617 weathering rates: clues from the Mackenzie River Basin, Canada. Geochim.
618 Cosmochim. Acta 67, 1305-1329, 2003.
619 Millot, R., Gaillardet, J., Dupré, B., Allègre, C.J., The global control of silicate
620 weathering rates and the coupling with physical erosion: new insights from
621 rivers of the Canadian Shield. Earth Planet. Sci. Lett. 196, 83-98, 2002.
622 Ministry of Environmental Protection of China, 2009. China Environmental Quality
623 Report 2008. China Environmental Sciences Press, Beijing. In Chinese.
624 Moon, S., Chamberlain, C.P., Hilley, G.E., New estimates of silicate weathering rates
625 and their uncertainties in global rivers. Geochim. Cosmochim. Acta 134, 257-
626 274, 2014.
627 Moon, S., Huh, Y., Qin, J., van Pho, N., Chemical weathering in the Hong (Red) River

basin: Rates of silicate weathering and their controlling factors. Geochim. Cosmochim. Acta 71, 1411-1430, 2007.

Moon, S., Huh, Y., Zaitsev, A., Hydrochemistry of the Amur River: Weathering in a Northern Temperate Basin. Aquat. Geochem., 15, 497-527, 2009.

Mortatti, J., Probst, J.L., Silicate rock weathering and atmospheric/soil CO_2 uptake in the Amazon basin estimated from river water geochemistry: seasonal and spatial variations. Chem. Geol.197, 177-196, 2003.

Négrel, P., Allègre, C.J., Dupré, B., Lewin, E., Erosion sources determined by inversion of major and trace element ratios and strontium isotopic ratios in river water: the Congo Basin Case. Earth Planet. Sci. Lett. 120, 59-76, 1993.

Noh, H., Huh, Y., Qin, J., Ellis, A., Chemical weathering in the Three Rivers region of Eastern Tibet. Geochim. Cosmochim. Acta 73, 1857-1877, 2009.

Oliva, P., Viers, J., Dupré B., Chemical weathering in granitic environments. Chem. Geol. 202, 225-256, 2003.

Pan, Y.,Wang, Y., Tang, G., Wu, D., Spatial distribution and temporal variations of atmospheric sulfur deposition in Northern China: insights into the potential acidification risks. Atmos. Chem. Phys. 13, 1675-1688, 2013.

Pepin, E., Guyot, J.L., Armijos, E., Bazan, H., Fraizy, P., Moquet, J.S., Noriega, L., Lavado, W., Pombosa, R. Vauchel, P., Climatic control on eastern Andean denudation rates (Central Cordillera from Ecuador to Bolivia). J. S. Am. Earth Sci. 44, 85-93, 2013.

Perrin, A.-S., Probst, A., Probst, J.-L., Impact of nitrogenous fertilizers on carbonate

650 dissolution in small agricultural catchments: Implications for weathering CO_2
651 uptake at regional and global scales. Geochim, Cosmochim. Acta 72, 3105-
652 3123, 2008.
653 Probst, A., Gh'mari, A.El., Aubert, D., Fritz, B., McNutt, R., Strontium as a tracer of
654 weathering processes in a silicate catchment polluted by acid atmospheric
655 inputs, Strengbach, France. Chem. Geol. 170, 203-219, 2000.
656 Raymo, M.E., Ruddiman,W.F., Tectonic forcing of late Cenozoic climate. Nature 359,
657 117-122, 1992.
658 Raymond, P. A., Oh, N.H., Turner, R.E., Broussard, W., Anthropogenically enhanced
659 fluxes of water and carbon from the Mississippi River. Nature 451, 449-452,
660 2008.
661 Regnier, P., Friedlingstein, P., Ciais, P., Mackenzie, F.T.,…Thullner. M.,
662 Anthropogenic perturbation of the carbon fluxes from land to ocean. Nature
663 Geosci. 6, 597-607. 2013.
664 Reuss, J.O., Cosby, B.J., Wright, RF., Chemical processes governing soil and water
665 acidification. Nature 329, 27-32, 1987.
666 Roy, S., Gaillardet, J., Allègre, C.J., Geochemistry of dissolved and suspended loads
667 of the Seine river, France: anthropogenic impact, carbonate and silicate
668 weathering. Geochim. Cosmochim. Acta 63, 1277-1292, 1999.
669 Ryu, J.S., Lee, K.S., Chang, H.W., Shin, H.S., Chemical weathering of carbonates and
670 silicates in the Han River basin, South Korea. Chem. Geol. 247, 66-80, 2008.
671 Semhi, K., Amiotte Suchet, P., Clauer, N., Probst, J.-L., Impact of nitrogen fertilizers

672 on the natural weathering-erosion processes and fluvial transport in the Garonne
673 basin. Appl. Geochem. 15 (6), 865-874, 2000.
674 Shi, C., Chemical characteristics and weathering of rivers in the Coast of Southeast
675 China (PhD Thesis). Institute of Geology and Geophysics, Chinese academy of
676 sciences, Beijing, China. pp, 1-100 (in Chinese with English abstract), 2014.
677 Shin, W.-J., Ryu, J.-S., Park, Y., Lee, K.-S., Chemical weathering and associated CO_2
678 consumption in six major river basins, South Korea. Geomorphology 129, 334-
679 341, 2011.
680 Shu, L.S., Zhou, X.M., Deng, P., Wang, B., Jiang, S.Y., Yu, J.H., Zhao, X.X.,
681 Mesozoic tectonic evolution of the Southeast China Block: New insights from
682 basin analysis. J. Asian Earth Sci. 34(3), 376-391, 2009.
683 Spence, J., Telmer, K., The role of sulfur in chemical weathering and atmospheric
684 CO_2 fluxes: Evidence from major ions, $\delta^{13}C_{DIC}$, and$\delta^{34}S_{SO4}$ in rivers of the
685 Canadian Cordillera. Geochim. Cosmochim. Acta 69, 5441-5458, 2005.
686 Stallard, R.F., Edmond, J.M., Geochemistry of the Amazon. Precipitation chemistry
687 and the marine contribution to the dissolved load at the time of peak discharge.
688 J. Geophys. Res., 86, 9844-9858, 1981.
689 U.S. Nat. Res. Council Comm., Basic Research Opportunities in Earth Science.
690 Washington, DC: Nat. Acad. 154 pp., 2001.
691 Viers, J., Dupré, B., Braun, J.J., Freydier, R., Greenberg, S., Ngoupayou, J.N.,
692 Nkamdjou, L.S., Evidence for non-conservative behavior of chlorine in humid
693 tropical environments. Aquat. Geochem. 7, 127-154, 2001.

694 Vries, W.D., Reinds, G.J. Vel E., Intensive monitoring of forest ecosystems in Europe.
695 2-Atmospheric deposition and its impacts on soil solution chemistry. For. Ecol.
696 Manage. 174, 97-115, 2003.
697 Wang, T.J., Jin, L.S., Li, Z.K., Lam K.S., A modeling study on acid rain and
698 recommended emission control strategies in China. Atmos. Environ. 34, 4467-
699 4477, 2000.
700 West, A.J., Galy, A., Bickle, M., Tectonic and climatic controls on silicate weathering.
701 Earth Planet. Sci. Lett. 235, 211-228, 2005.
702 Wu, W., Zheng, H., Yang, J., Luo, C., Zhou, B., Chemical weathering, atmospheric
703 CO_2 consumption, and the controlling factors in a subtropical metamorphic-
704 hosted watershed. Chem. Geol. 356, 141-150, 2013.
705 Xiang, L., Study on Coupling between Water and Carbon of Artificial Forests
706 Communities in Subtropical Southern China. Master Dissertation, Institute of
707 Geographical Sciences and Natural Sources, Chinese Academy of Sciences,
708 China (in Chinese), 2006.
709 Xu, H., Bi, X-H., Feng, Y-C., Lin, F-M., Jiao, L., Hong, S-M., Liu, W-G., Zhang, X.-
710 Y., Chemical composition of precipitation and its sources in Hangzhou, China.
711 Environ. Monit. Assess. 183:581-592, 2011.
712 Xu, Y., Wang C.Y., Zhao T., Using detrital zircons from river sands to constrain major
713 tectono-thermal events of the Cathaysia Block, SE China. J. Asian Earth Sci.
714 124, 1-13, 2016.
715 Xu, Z., Liu, C.-Q., Chemical weathering in the upper reaches of Xijiang River

716 draining the Yunnan-Guizhou Plateau, Southwest China. Chem. Geol. 239, 83-
717 95, 2007.
718 Xu, Z., Liu, C.-Q., Water geochemistry of the Xijiang basin rivers, South China:
719 Chemical weathering and CO_2 consumption. Appl. Geochem. 25, 1603-1614,
720 2010.
721 Yoshimura, K., Nakao, S., Noto, M., Inokura, Y., Urata, K., Chen, M., Lin, P.W.,
722 Geochemical and stable isotope studies on natural water in the Taroko Gorge
723 karst area, Taiwan - chemical weathering of carbonate rocks by deep source
724 CO_2 and sulfuric acid. Chem. Geol. 177, 415–430, 2001.
725 Zhang, M., Wang, S., Wu, F., Yuan, X., Zhang, Y., Chemical compositions of wet
726 precipitation and anthropogenic influences at a developing urban site in
727 southeastern China. Atmos. Res. 84, 311-322, 2007a.
728 Zhang, S.R., Lu, X. X., Higgitt, D. L., Chen, C.T.A., Sun, H.-G., Han, J.T., Water
729 chemistry of the Zhujiang (Pearl River): Natural processes and anthropogenic
730 influences. J. Geophys. Res. 112, F01011, 2007b.
731 Zhao, W., An analysis on the changing trend of acid rain and its causes in Fujian
732 Province. Fujian Geogr. 19, 1-5 (in Chinese), 2004.
733 Zhou, X.M., Li, W.X., Origin of Late Mesozoic igneous rocks in Southeastern China:
734 Implications for lithosphere subduction and underplating of mafic magmas.
735 Tectonophysics 326(3-4), 269-287, 2000.
736 Zhou, X.M., Sun, T., Shen, W.Z., et al., Petrogenesis of Mesozoic granitoids and
737 volcanic rocks in South China: A response to tectonic evolution. Episodes 29(1),

738 26-33, 2006.

739 ZJBGMR: Zhejiang Bureau of Geology and Mineral Resources, Regional Geology of

740 Zhejiang Province. Geol. Publ. House, Beijing, p. 617 (in Chinese with English

741 abstract), 1989.

Table 1 Chemical and carbon isotopic compositions of river waters in the Southeast Coastal Rivers Basin (SECRB) of China.

Rivers	Sample number	Date (M/D/Y)	pH	T ℃	EC μs cm^{-1}	Na^+ μM	K^+ μM	Mg^{2+} μM	Ca^{2+} μM	F^- μM	Cl^- μM	NO_3^- μM	SO_4^{2-} μM	HCO_3^- μM	SiO_2 μM	TZ^+ μEq	TZ^- μEq	NICB %	$\delta^{13}C$ ‰	TDS mg l^{-1}
Qiantang*	1	07-8-10	7.42	28.78	190	347	197	106	473	12.0	303	62.6	147	1130	148	1703	1789	-5.0	-19.0	144
	2	07-9-10	7.60	23.84	146	87.5	204	80.9	496	11.7	75.2	124	121	907	156	1446	1348	6.7	-19.8	119
	3	07-9-10	7.37	27.83	308	555	233	208	698	41.8	312	223	437	1170	170	2601	2579	0.9	-17.8	204
	4	07-10-10	7.27	26.28	177	176	135	116	544	15.7	151	142	170	985	175	1632	1618	0.8	-19.3	135
	5	07-10-10	7.05	24.15	123	130	101	66.2	349	17.7	94.3	124	157	529	169	1061	1061	0.0	-18.7	91.2
	6	07-10-10	7.24	23.75	140	97.6	69.7	81.0	451	20.0	62.1	109	204	703	164	1231	1282	-4.2	-21.3	106.6
	7	07-11-10	7.40	23.23	107	92.5	70.5	68.3	327	14.9	74.9	104	147	486	156	954	960	-0.6	-21.0	82.2
	8	07-11-10	7.16	27.61	281	361	87.5	128	469	26.8	245	191	239	810	179	1642	1724	-5.0	-12.9	137.5
	9	07-11-10	7.02	26.48	140	275	120	60.7	319	36.2	199	150	180	437	236	1155	1146	0.8	-13.9	100.2
	10	07-12-10	7.05	24.24	99	205	114	58.3	285	14.6	191	114	132	305	278	1005	874	13.1	-20.9	85.4
	11	07-12-10	7.05	27.01	102	123	133	49.8	284	18.6	86.5	123	144	377	183	924	874	5.4	-19.2	79.4
	12	07-12-10	7.99	24.18	260	50.0	85.4	212	993	-	66.8	153	235	1822	172	2546	2512	1.4	-17.6	205.2
	13	07-12-10	7.86	24.59	231	43.5	88.4	189	859	-	55.1	97.6	169	1763	170	2228	2253	-1.1	-18.7	185.4
	14	07-12-10	7.69	22.66	131	44.1	81.0	113	458	-	19.1	95.2	107	920	143	1266	1248	1.4	-18.1	106.8
	15	07-12-10	7.65	24.48	106	61.1	98.3	87.9	335	-	37.2	68.3	112	663	164	1005	992	1.4	-18.6	87.3
	16	07-12-10	7.46	23.68	125	64.3	108	117	406	-	25.9	75.0	174	687	164	1218	1136	6.7	-20.0	98.8
	17	07-13-10	7.33	24.08	139	59.8	116	136	429	-	29.6	80.4	209	752	162	1305	1281	1.9	-20.8	108.1
	18	07-10-10	7.27	25.74	141	163	114	69.6	396	27.3	126	148	161	597	153	1209	1195	1.1	-21.0	101.0
Cao'e	19	07-16-10	7.17	22.27	108	212	86.3	69.4	183	5.1	151	148	114	384	216	803	912	-13.5	-21.2	79.1
	20	07-16-10	7.06	26.57	182	401	77.6	145	275	18.3	269	185	245	534	215	1318	1478	-12.2	-20.5	116.9
	21	07-16-10	7.14	27.26	171	333	91.3	164	362	18.1	224	194	207	658	225	1475	1490	-1.0	-20.9	123.3
	22	07-16-10	7.08	27.17	173	346	94.4	168	364	18.8	247	200	211	656	222	1506	1526	-1.3	-13.0	125.2
Ling	23	07-15-10	7.07	24.14	52	164	42.9	34.9	140	4.9	40.7	61.5	68.3	277	190	558	516	7.6	-12.8	52.1
	24	07-15-10	7.02	26.04	74	169	92.0	34.2	150	6.4	87.0	77.3	92.8	272	196	629	622	1.1	-20.8	59.5
	25	07-16-10	7.34	25.03	92	159	80.1	47.3	235	19.3	78.0	71.4	105	455	187	804	815	-1.4	-22.5	73.9
	26	07-16-10	7.40	26.75	113	216	77.8	57.1	249	20.2	133	90.0	115	494	196	905	946	-4.5	-12.7	82.8
	27	07-16-10	7.39	26	89	174	86.4	56.4	209	9.0	99.3	78.4	99.9	420	199	792	798	-0.8	-14.0	72.7
	28	07-15-10	6.79	22.33	75	159	82.7	44.1	143	-	107	61.8	83.4	306	144	616	641	-4.1	-21.1	56.5
	29	07-15-10	8.24	27.15	129	228	92.1	83.1	317	17.2	177	90.5	120	641	194	1120	1148	-2.5	-19.2	97.8
Ou	30	07-13-10	8.08	28.45	48	95.2	107	38.4	92.1	15.2	31.8	43.3	47.4	291	221	463	461	0.4	-21.7	50.6
	31	07-13-10	6.71	22.97	32	60.7	106	12.6	65.0	10.8	28.9	45.0	48.9	158	169	322	329	-2.2	-23.8	36.9
	32	07-13-10	7.18	27.59	73	107	127	36.2	175	4.3	57.1	111	92.0	283	210	655	634	3.2	-23.4	62.9
	33	07-13-10	6.94	24.2	44	76.9	112	20.0	99.1	10.9	27.9	63.1	58.6	249	184	427	457	-7.0	-22.5	47.5
	34	07-14-10	7.16	27.45	90	187	127	41.2	199.5	17.0	85.6	102	116	367	251	796	787	1.1	-22.4	76.5
	35	07-14-10	6.97	24.56	54	105	50.9	29.2	122	12.2	46.1	67.8	73.1	218	193	460	478	-4.1	-22.5	47.9
	36	07-14-10	6.82	21.12	31	76.4	133	12.7	74.5	7.7	20.7	36.8	49.1	192	162	383	348	9.3	-	39.5
	37	07-14-10	6.82	23.69	45	89.5	105	19.0	97.8	10.6	39.6	52.8	59.1	231	185	428	441	-3.0	-22.9	46.2
	38	07-15-10	6.92	24.69	37	100	89.3	21.1	49.7	1.7	36.9	45.5	52.7	153	202	331	341	-2.9	-	38.9
	39	07-15-10	6.90	23.86	35	92.2	92.0	19.8	61.4	1.9	43.9	47.9	55.5	139	193	347	342	1.4	-22.3	38.5
	40	07-15-10	7.09	25.56	47	117	112	25.7	83.4	8.0	52.4	63.1	57.4	232	193	447	462	-3.3	-22.5	48.1
	41	07-14-10	6.97	24.25	53	102	107	27.6	119	13.4	43.5	59.4	73.2	277	183	502	526	-4.9	-13.7	52.3

Feiyun	42	07-17-10	7.28	25.19	38	94.0	81.7	24.0	75.6	11.4	59.9	45.7	51.9	149	151	375	358	4.5	-	37.2
	43	07-17-10	7.08	25.61	46	101	79.9	33.9	93.4	4.6	66.2	55.1	52.8	223	151	435	450	-3.3	-23.7	43.5
Jiaoxi	44	07-17-10	7.52	26.92	47	116	81.5	25.2	92.0	4.1	73.3	80.3	25.0	226	151	432	430	0.5	-23.4	43.0
	45	07-17-10	7.45	27.46	61	152	90.2	34.2	119	-	136	59.8	53.5	238	184	548	542	1.2	-23.1	51.8
	46	07-18-10	6.90	27.66	53	127	88.1	33.4	94.4	7.0	123	93.1	30.4	209	177	471	486	-3.3	-14.4	47.4
Huotong	47	07-18-10	7.34	24	43	116	78.8	26.1	58.4	5.4	68.7	49.7	20.1	197	190	364	355	2.3	-22.8	39.6
Ao	48	07-19-10	7.24	31.44	124	294	121	102	209	24.3	204	73.6	52.0	717	370	1036	1100	-6.1	-19.4	105.4
	49	07-19-10	7.13	27.82	46	109	96.3	30.0	73.8	-	72.0	51.3	22.5	234	236	413	402	2.6	-	46.2
	50	07-18-10	6.98	28.65	53	140	88.4	40.8	100	3.0	82.9	58.6	20.9	294	233	511	477	6.6	-22.3	52.2
Min	51	07-27-10	7.11	28.4	42	116	92.0	40.5	119	18.0	43.9	35.5	26.0	382	182	526	513	2.4	-19.4	52.7
	52	07-27-10	7.17	30	51	102	97.9	41.7	107	4.6	29.4	45.3	35.0	350	221	496	495	0.2	-	53.3
	53	07-27-10	7.08	29.4	99	214	92.7	46.4	126	18.4	50.1	39.8	118	327	154	651	654	-0.4	-20.8	74.0
	54	07-27-10	7.06	29.1	44	107	99.6	28.1	114	16.4	18.7	36.4	44.3	305	265	491	449	8.5	-17.6	53.6
	55	07-27-10	7.42	29.4	57	139	93.7	49.8	113	3.1	67.1	56.3	26.6	384	236	558	561	-0.5	-16.4	58.6
	56	07-27-10	7.12	27.8	51	103	91.0	50.8	106	4.7	82.8	35.1	63.5	249	225	507	494	2.5	-	51.3
	57	07-27-10	7.08	27.5	40	125	45.0	36.8	107	12.1	43.6	44.5	29.3	288	211	457	435	5.0	-21.1	47.4
	58	07-27-10	6.99	27.2	52	121	98.0	42.4	115	16.7	87.1	36.6	70.9	277	228	535	542	-1.4	-11.4	55.3
	59	07-27-10	6.87	29	59	154	91.4	59.4	124	16.5	77.8	36.7	88.3	272	222	612	563	8.0	-20.3	57.2
	60	07-27-10	7.31	27.1	78	109	92.1	59.1	181	21.2	123	37.5	78.4	355	202	682	672	1.4	-18.7	63.1
	61	07-27-10	7.22	27.8	37	122	83.3	52.8	142	17.4	111	37.3	80.4	288	221	596	597	-0.2	-22.3	58.1
	62	07-27-10	7.16	28.1	58	104	83.3	59.3	163	24.0	34.6	34.5	118	294	214	632	599	5.2	-13.4	59.5
	63	07-27-10	7.26	28.3	87	139	86.1	60.9	191	14.8	48.0	93.0	109	347	226	729	707	3.0	-21.4	68.6
	64	07-27-10	7.00	28.8	87	127	93.1	58.7	195	6.6	59.8	81.1	60.9	480	232	729	743	-2.0	-11.0	74.0
	65	07-28-10	6.97	27.9	37	163	82.1	52.2	140	20.2	53.1	60.0	106	306	221	630	632	-0.2	-	61.9
	66	07-13-10	7.07	27.96	59	91.9	110	40.0	127	24.8	62.0	79.3	62.3	249	228	535	515	3.8	-	54.8
	67	07-28-10	7.12	29.7	38	108	93.4	45.9	133	12.4	48.3	34.0	56.6	368	220	560	564	-0.7	-	57.7
	68	07-27-10	7.03	29.9	62	128	96.7	57.6	148	23.3	81.6	36.8	74.1	374	203	635	641	-0.9	-12.4	61.7
	69	07-27-10	7.01	28.8	60	102	89.1	73.6	138	9.6	50.6	74.1	32.7	417	233	615	607	1.3	-21.0	62.3
	70	07-27-10	7.06	26.5	37	93.5	93.1	34.7	87.3	-	26.6	34.8	37.1	312	222	431	448	-3.9	-13.1	49.1
	71	07-27-10	7.09	26.5	25	62.6	92.7	27.0	61.5	4.7	21.5	18.6	43.4	191	154	332	318	4.2	-16.0	35.3
	72	07-28-10	7.07	30.1	39	76.3	87.9	35.1	87.6	7.4	43.1	36.6	35.5	266	175	409	416	-1.7	-19.4	43.5
	73	07-27-10	7.01	28.7	47	84.9	95.4	56.7	106	12.7	51.8	49.2	57.2	315	211	506	531	-4.8	-	53.8
	74	07-27-10	6.85	28.7	50	93.6	85.9	52.4	107	14.1	62.8	57.5	57.0	252	217	498	487	2.2	-19.9	50.9
	75	07-27-10	7.11	29.7	69	117	85.2	73.4	159	7.6	63.7	75.2	47.4	418	230	666	652	2.2	-22.2	65.0
	76	07-28-10	6.93	28.9	59	112	88.0	61.8	122	6.0	57.4	89.3	42.0	349	224	568	580	-2.2	-22.0	58.8
	77	07-21-10	7.76	32.4	51.2	163	85.5	52.8	151	20.2	55.3	70.3	78.6	372	175	656	655	0.3	-12.5	61.8
	78	07-28-10	7.29	26.8	106	129	75.3	84.0	321	24.0	56.2	41.0	166	599	202	1013	1028	-1.4	-16.3	90.3
	79	07-21-10	7.09	26.96	56	112	87.6	37.1	129	4.5	51.5	44.9	61.9	327	276	531	547	-2.9	-22.2	59.1
	80	07-21-10	7.64	33.37	83	114	96.2	60.6	151	16.7	53.0	40.6	102	371	242	633	670	-5.8	-12.8	66.2
	81	07-21-10	7.83	31.27	65	131	102	52.7	141	16.1	45.3	49.7	91.8	324	239	620	603	2.8	-13.4	61.8
	82	07-21-10	6.84	28.35	66	132	101	52.5	141	5.8	63.8	54.1	91.6	304	243	621	606	2.5	-22.7	61.5
	83	07-21-10	7.42	30.7	98	217	113	59.2	210	18.4	98.7	63.5	84.7	496	320	868	827	4.6	-18.9	84.5
	84	07-27-10	7.26	26.3	46	104	102	29.7	121	3.6	55.2	51.9	55.5	294	193	507	512	-0.9	-21.6	51.9
	85	07-27-10	7.07	25.4	30	73.3	99.2	19.6	78.8	-	22.9	40.0	49.2	203	170	369	365	1.3	-21.1	39.8
	86	07-27-10	7.50	27.3	45	102	102	26.5	114	2.4	35.1	39.7	57.2	260	217	484	449	7.3	-15.7	49.6
	87	07-27-10	7.47	26.9	51	141	100	43.6	109	7.9	79.7	42.4	57.7	311	217	547	548	-0.3	-20.1	55.6

	88	07-19-10	7.99	31.74	63	167	96.5	33.5	115	8.0	105	35.5	38.1	331	218	561	548	2.3	-13.5	55.9
	89	07-21-10	6.77	28.19	65	132	93.6	56.0	145	15.6	60.6	78.8	75.4	333	243	627	624	0.5	-22.6	63.3
Jin	90	07-27-10	7.36	25.8	128	126	94.8	88.9	406	22.9	51.4	39.4	229	595	208	1211	1143	5.6	-20.7	100
	91	07-27-10	7.40	26.9	123	143	103	82.7	347	21.0	83.5	203	182	463	226	1105	1115	-0.9	-21.3	98.4
	92	07-27-10	7.00	27.4	88	170	98.8	56.8	205	7.2	137	117	106	327	205	793	792	0.1	-22.5	71.8
	93	07-27-10	7.32	28.7	73	201	116	87.1	318	20.0	93.5	41.5	189	508	267	1128	1020	9.6	-21.7	95.3
Jiulong	94	07-30-10	6.50	23.47	29	72.3	92.4	22.8	59.8	12.4	25.1	27.0	50.0	189	213	330	341	-3.4	-18.1	40.1
	95	07-30-10	7.06	29.35	120	136	96.9	106	339	5.1	67.7	66.3	249	469	202	1124	1100	2.1	-20.8	94.2
	96	07-30-10	7.45	27.6	104	79.5	97.5	106	363	14.4	70.7	50.0	99.9	729	184	1116	1049	6.0	-18.9	93.7
	97	07-31-10	7.36	26.59	139	140	100	142	432	15.5	79.6	78.3	274	573	196	1388	1278	8.0	-19.7	108.8
	98	07-31-10	7.72	26.18	88	77.6	96.2	69.0	313	19.9	39.7	34.6	63.8	731	251	938	933	0.5	-18.4	89.4
	99	07-30-10	7.43	26.96	119	200	93.8	100.2	298	19.9	122	80.5	225	387	202	1091	1040	4.7	-20.5	89.5
	100	07-28-10	7.41	26.66	112	173	97.9	94.4	286	46.1	118	152	201	364	207	1033	1036	-0.3	-20.9	92.2
	101	07-29-10	7.16	29.35	82	151	110	55.4	178	4.9	71.2	170	53.2	385	305	727	732	-0.7	-21.2	76.1
	102	07-29-10	7.10	28.9	100	222	98.3	49.4	249	3.6	126	157	52.7	532	303	917	920	-0.3	-21.7	90.0
	103	07-28-10	7.20	31.15	138	339	111	81.2	277	9.2	280	285	88.6	515	317	1165	1256	-7.8	-19.0	112
	104	07-28-10	7.16	27.09	101	261	95.8	81.7	235	40.3	173	80.1	174	291	136	990	892	9.9	-24.3	75.4
Zhang	105	07-28-10	8.08	30.6	93	195	96.1	61.1	167	16.8	157	193	55.2	281	288	748	741	0.9	-21.5	73.8
Dongxi	106	07-28-10	7.20	30.9	78	263	99.0	41.5	115	14.5	238	65.3	30.0	283	309	675	646	4.4	-20.8	66.7
Huangang	107	07-28-10	7.40	30.5	99	253	85.6	53.0	154	7.7	190	63.5	56.4	460	278	754	827	-9.6	-20.0	77.4
Han	108	07-31-10	7.31	27.1	68	136	61.5	45.2	195	16.1	37.7	45.3	93.7	345	218	678	615	9.2	-21.9	62.0
	109	07-30-10	7.38	26.94	88	116	103	63.6	265	6.4	53.4	72.2	84.9	584	244	876	879	-0.4	-20.4	83.7
	110	07-30-10	6.66	25.55	71	114	96.2	47.6	168	8.0	56.9	54.6	143	230	203	642	628	2.2	-17.9	59.7
	111	07-30-10	6.66	27.76	83	135	104	63.8	203	8.6	54.5	74.9	173	302	336	774	777	-0.4	-20.6	78.7
	112	07-30-10	7.31	30.81	56	168	74.0	39.1	118	13.5	62.9	44.4	81.4	237	245	556	507	8.8	-21.4	54.6
	113	07-31-10	7.28	28.73	98	137	99.3	85.6	270	9.2	88.8	59.1	118	565	233	948	949	-0.1	-19.7	86.6
	114	07-31-10	7.27	31.42	123	193	105	98.2	319	20.7	120	102	157	570	229	1132	1107	2.2	-19.7	98.2
	115	07-30-10	7.43	29.89	85	115	97.5	65.5	244	6.5	46.5	58.6	103	511	251	832	822	1.1	-20.8	79.3
	116	07-31-10	7.61	30.98	99	123	104	85.9	264	5.6	58.8	90.9	108	588	98	926	952	-2.9	-20.0	79.4
	117	07-31-10	7.31	29.96	93	151	103	78.1	250	15.4	68.0	99.1	173	379	233	909	891	1.9	-21.9	81.8
	118	07-31-10	7.35	28.4	2	233	84.2	101	323	12.8	84.0	101	203	460	229	1165	1051	9.8	-21.1	94.7
	119	07-31-10	7.67	30.38	93	136	87.8	73.6	231	16.4	64.6	94.4	184	382	226	834	909	-9.1	-20.8	80.5
Rong	120	07-30-10	7.57	31.83	68	193	79.1	50.3	146	16.4	192	84.0	31.5	344	309	664	683	-2.8	-20.3	65.8
	121	07-30-10	6.96	30.62	94	509	103	56.1	213	15.9	511	78.5	82.3	379	222	1150	1133	1.5	-20.0	94.4

TZ^+ is the total cationic charge; TZ^- is the total anionic charge; NICB is the normalized inorganic charge balance and TDS is the total dissolved solid. *data of major ion composition from the previous work by Liu et al. 2016.

Table 2 Chemical compositions of precipitation at different sites located within the studied area (in μmol l^{-1} and molar ratio).

Province	Location	pH	F^-	Cl^-	NO_3^-	SO_4^{2-}	NH_4^+	K^+	Na^+	Ca^{2+}	Mg^{2+}	NO_3/Cl	SO_4/Cl	K/Cl	Na/Cl	Ca/Cl	Mg/Cl	Reference
Zhejiang	Hangzhou	4.5	5.76	13.9	38.4	55	79.9	4.18	12.2	26	3.53	2.76	3.96	0.3	0.88	1.87	0.25	Xu et al., 2011
	Jinhua	4.54	9.05	8.51	31.2	47.6	81.1	4.73	6.27	24	1.73	3.67	5.59	0.56	0.74	2.81	0.2	Zhang et al., 2007
Fujian	Nanping	4.81	0.8	5.8	26.6	18.3	38	4.9	5.4	12.9	2.7	4.59	3.16	0.84	0.93	2.22	0.47	Cheng et al., 2011
	Fuzhou		5.26	21.4	24.9	48.5	78.1	4.1	2.61	32.7	1.25	1.16	2.26	0.19	0.12	1.53	0.06	Zhao, 2004
	Xiamen	4.57	15.3	23.7	22.1	31.3	37.7	3.58	36.1	21.5	4.94	0.93	1.32	0.15	1.52	0.91	0.21	Zhao, 2004
Average												2.62	3.26	0.41	0.84	1.87	0.24	

Table 3 Contribution of each reservoir, fluxes, chemical weathering and associated CO_2 consumption rates for the major rivers and their main tributaries in the SECRB.

Major river	Tributaries	Location	Discharge	Area	Runoff	Contribution (%)				Fluxes (10^6 ton a^{-1})		Weathering rate (ton $km^{-2}a^{-1}$)				CO_2 consumption rate (10^3 mol km^{-2} a^{-1})			
			10^9 m^3a^{-1}	10^3 km^2	mm a^{-1}	Rain	Anth.	Sil.	Carb.	SWF	CWF	Cat_{sil}[a]	SWR[b]	CWR[b]	TWR[b]	CSW[c]	CCW[c]	SSW[d]	SSW[e]
Qiantang		Fuyang	43.81	38.32	1143	9	14	23	54	0.66	1.74	6.8	17.3	45.3	62.6	223	459	195	184
	Fenshui	Tonglu	2.726	3.100	879	7	14	18	62	0.05	0.16	5.5	14.7	52.1	66.8	167	530	152	146
Cao'e		Huashan	2.610	3.043	858	7	23	26	44	0.06	0.11	6.8	18.2	35.4	53.5	269	369	240	229
Ling		Linhai	5.400	6.613	817	9	22	24	45	0.09	0.17	4.7	14.2	26.1	40.3	167	267	143	133
	Yonganxi	Baizhiao	3.184	2.475	1286	14	15	50	21	0.06	0.03	9.1	24.2	11.7	35.9	350	119	255	216
	Shifengxi	Shaduan	1.731	1.482	1168	11	19	35	36	0.03	0.04	7.6	21.4	24.5	45.9	304	249	249	227
Ou		Hecheng	20.65	13.45	1536	20	6	56	18	0.36	0.13	10.1	26.9	9.9	36.9	360	101	228	174
	Haoxi	Huangdu	1.809	1.270	1447	16	8	46	30	0.04	0.02	9.9	27.9	19.0	46.9	336	192	246	210
	Xiaoxi	Jupu	5.116	3.336	1534	23	0	74	4	0.09	0.01	11.4	26.4	1.8	28.2	391	18	202	125
	Nanxi	Yongjiashi	1.799	1.273	1413	21	9	63	7	0.03	0.00	10.0	26.3	3.3	29.6	360	34	200	135
Huotong		Yangzhong	3.470	2.082	1667	22	18	54	5	0.06	0.00	8.3	27.3	2.1	29.4	305	24	129	59
Ao		Lianjiang	2.770	3.170	874	17	17	48	17	0.05	0.02	5.1	17.3	5.4	22.7	188	56	122	95
Min		Zhuqi	84.59	54.50	1552	15	10	48	27	1.80	0.94	10.3	33.0	17.3	50.2	390	180	292	252
	Futun	Yangkou	22.53	12.67	1778	15	14	49	22	0.45	0.21	12.0	35.8	16.2	52.0	460	171	336	286
	Shaxi	Shaxian	12.87	9.922	1297	13	9	42	36	0.26	0.21	8.4	26.5	21.7	48.1	315	222	249	223
	Jianxi	Qilijie	24.91	14.79	1685	16	10	45	29	0.48	0.26	9.6	32.2	17.4	49.6	350	185	250	210
	Youxi	Youxi	5.237	4.450	1177	15	8	46	31	0.11	0.07	7.4	24.5	15.0	39.5	272	156	205	178
	Dazhangxi	Yongtai	4.205	4.034	1042	15	21	47	17	0.08	0.03	6.6	20.2	7.1	27.4	242	73	163	131
Jin	Xixi	Anxi	3.004	2.466	1218	9	10	29	52	0.06	0.10	7.9	24.4	42.2	66.6	284	430	247	232
	Dongxi	Honglai	2.236	1.704	1312	12	22	28	38	0.04	0.04	6.8	22.9	25.6	48.5	226	263	178	158
Jiulong		Punan	10.20	8.49	1201	13	14	28	45	0.19	0.29	7.3	22.2	34.0	56.2	263	351	209	188
	Xi'xi	zhengdian	4.080	3.420	1193	10	32	25	33	0.10	0.11	8.0	30.7	30.9	61.6	288	317	227	203
Zhang		Yunxiao	1.011	1.038	974	16	25	29	29	0.02	0.01	5.1	21.9	14.1	36.0	174	146	114	90
Dongxi		Zhao'an	1.176	0.955	1231	16	41	26	17	0.03	0.01	5.8	28.7	10.2	38.9	187	107	93	55
Huanggang		Raoping	1.637	1.621	1010	15	30	34	21	0.04	0.02	6.0	22.8	11.1	33.9	227	115	145	112
Han		Chao'an	24.75	29.08	851	16	7	38	39	0.49	0.50	5.4	17.0	17.0	34.0	208	176	156	135

Ding	Xikou	11.14	9.228	1207	17	6	46	32	0.31	0.18	9.0	33.3	19.1	52.4	341	196	249	212
Mei	Hengshan	10.29	12.95	794	12	13	31	44	0.21	0.32	5.7	16.6	24.5	41.1	212	252	173	157
Whole SECRB		207	167	1240					3.95	4.09	7.8	23.7	24.5	48.1	287	251	218	191

[a] Cat_{sil} are calculated based on the sum of cations from silicate weathering.

[b] SWR, CWR and TWR represent silicate weathering rates (assuming all dissolved silica is derived from silicate weathering), carbonate weathering rates and total weathering rates, respectively.

[c] CO_2 consumption rate with assumption that all the protons involved in the weathering reaction are provided by carbonic acid.

[d] Estimated CO_2 consumption rate by silicate weathering when H_2SO_4 from acid precipitation is taken into account.

[e] Estimated CO_2 consumption rate by silicate weathering when H_2SO_4 and HNO_3 from acid precipitation is taken into account.

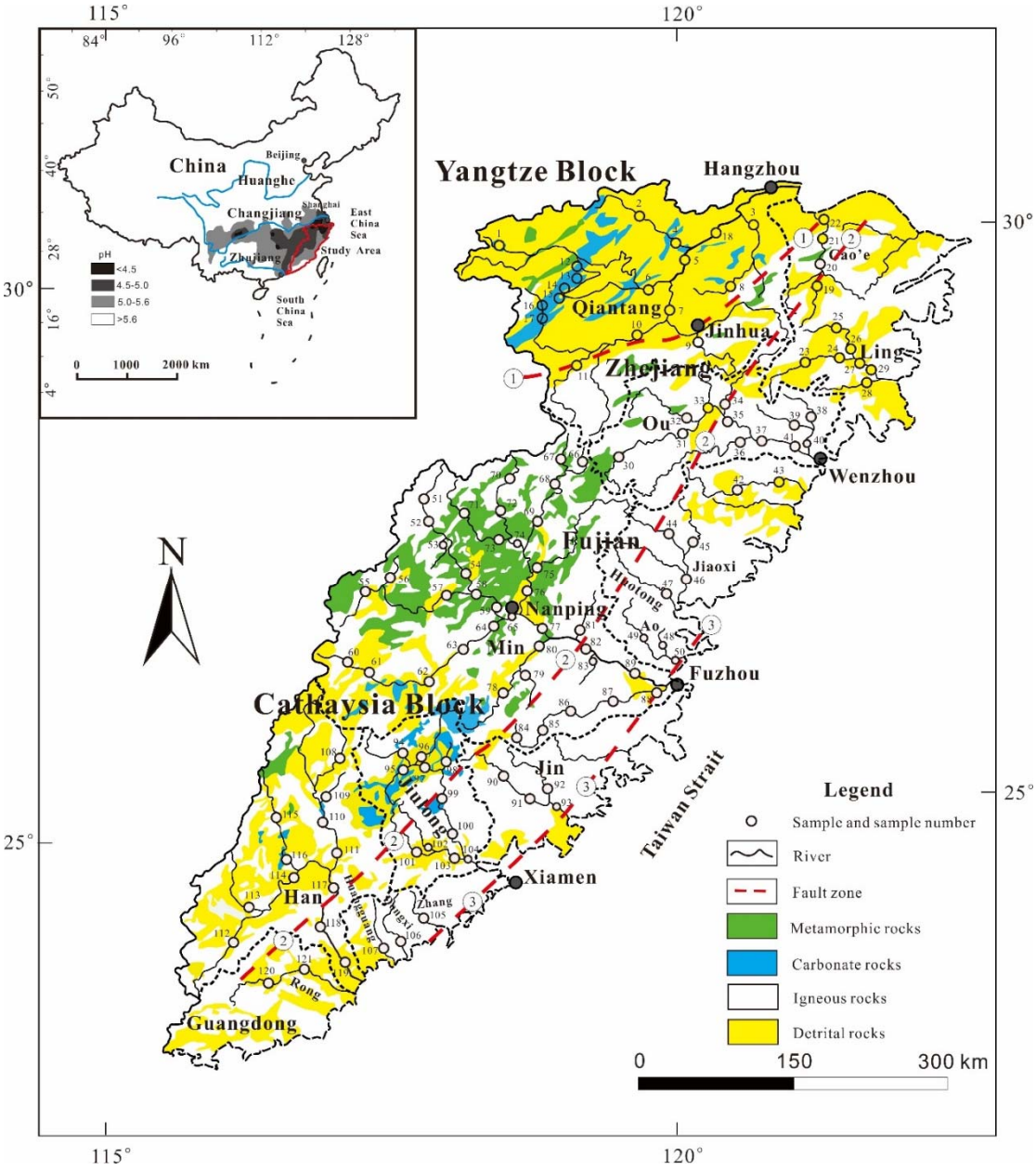

Fig. 1. Sketch map showing the lithology, sampling locations, and sample number of the SECRs drainage basin, and regional rain water pH ranges are shown in the sketch map at the upper-left. (modified from Zhou and Li, 2000; Shu et al., 2009; Xu et al., 2016, rain water acidity distribution of China mainland is from State Environmental Protection Administration of China). ①Shaoxing-Jiangshan fault zone; ②Zhenghe-Dapu fault zone; ③Changle-Nanao fault zone. The figure was created by CorelDraw software version 17.1.

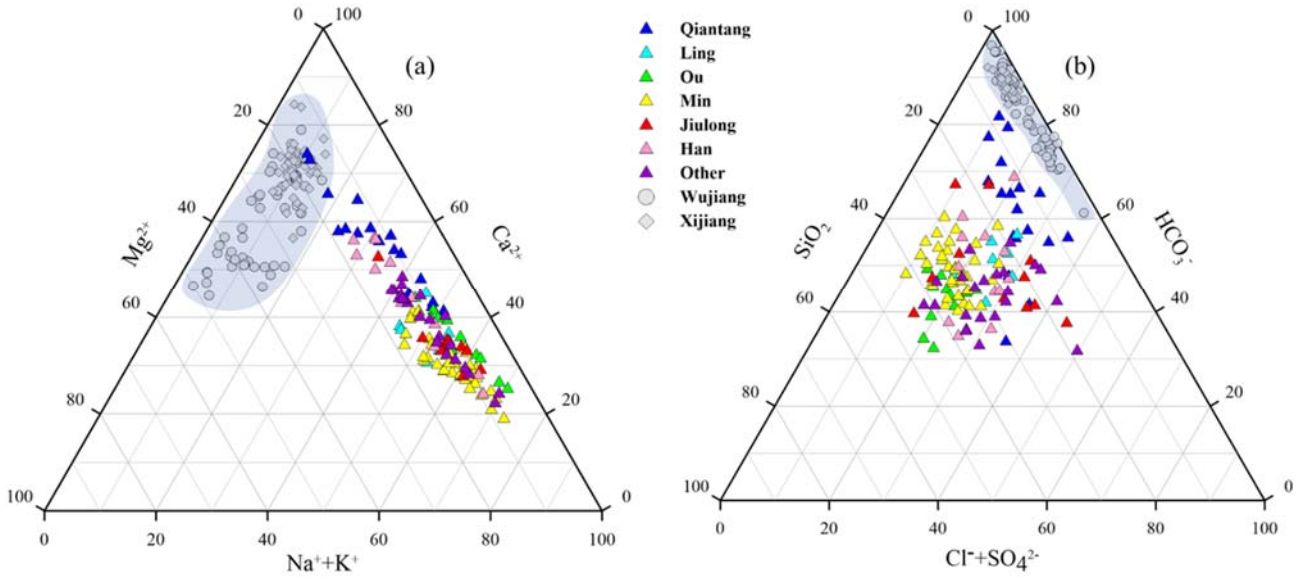

Fig. 2. Ternary diagrams showing cations (a), anions and dissolved SiO_2 (b) compositions of river waters in the SECRB. Chemical compositions from case studies of rivers draining carbonate rocks (the Wujiang and the Xijiang) are also shown for comparison (data from Han and Liu 2004; Xu and Liu 2007, 2010)

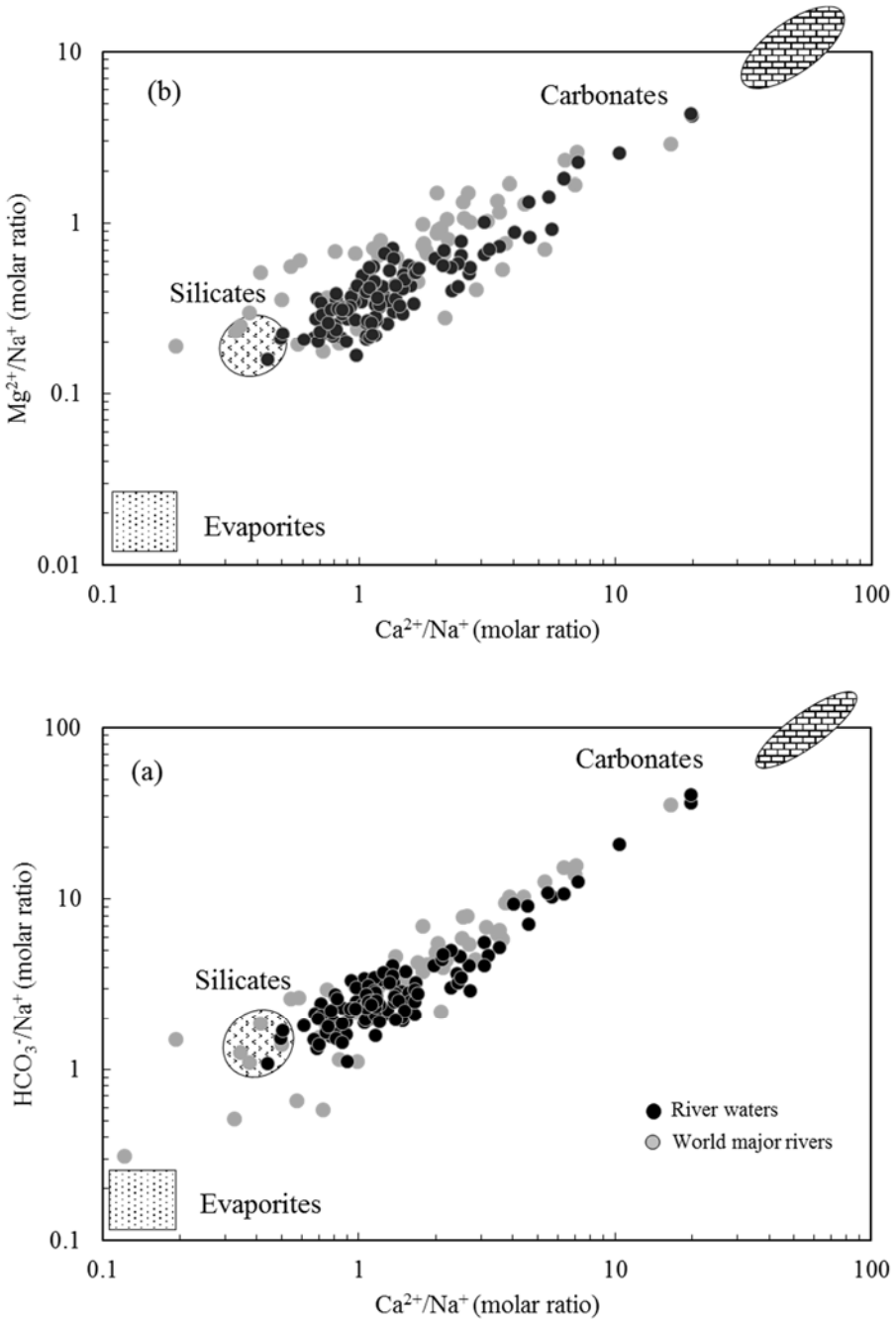

Fig. 3. Mixing diagrams using Na-normalized molar ratios: HCO_3^-/Na^+ *vs.* Ca^{2+}/Na^+ (a) and Mg^{2+}/Na^+ *vs.* Ca^{2+}/Na^+ (b) for the SECRB. The samples mainly cluster on a mixing line between silicate and carbonate end-members. Data for world major rivers are also plotted (data from Gaillardet et al. 1999).

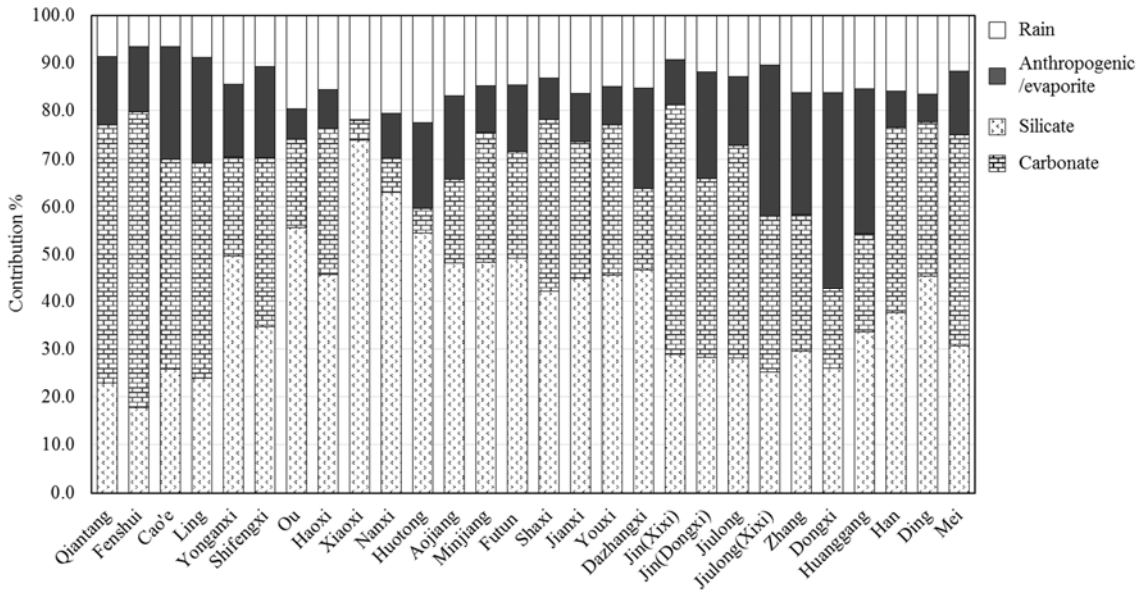

Fig. 4. Calculated contributions (in %) from the different reservoirs to the total cationic load for major rivers and their main tributaries in the SECRB. The cationic load is equal to the sum of Na^+, K^+, Ca^{2+} and Mg^{2+} from the different reservoirs.

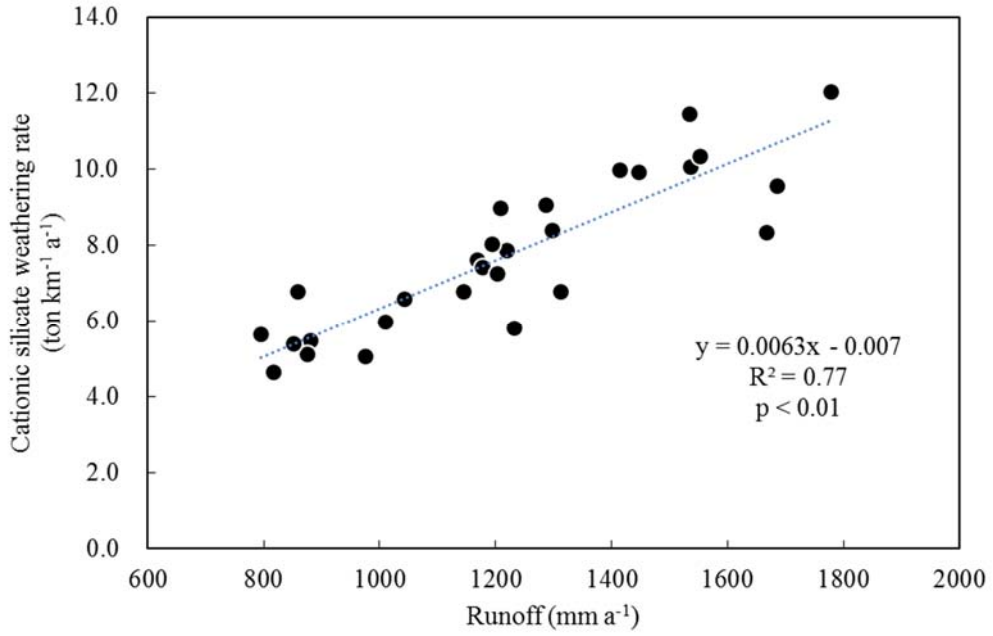

Fig. 5. Plots of the cationic-silicate weathering rate (Cat_{sil}) vs. runoff for the SECRB, showing that the silicate weathering rates is controlled by the runoff.

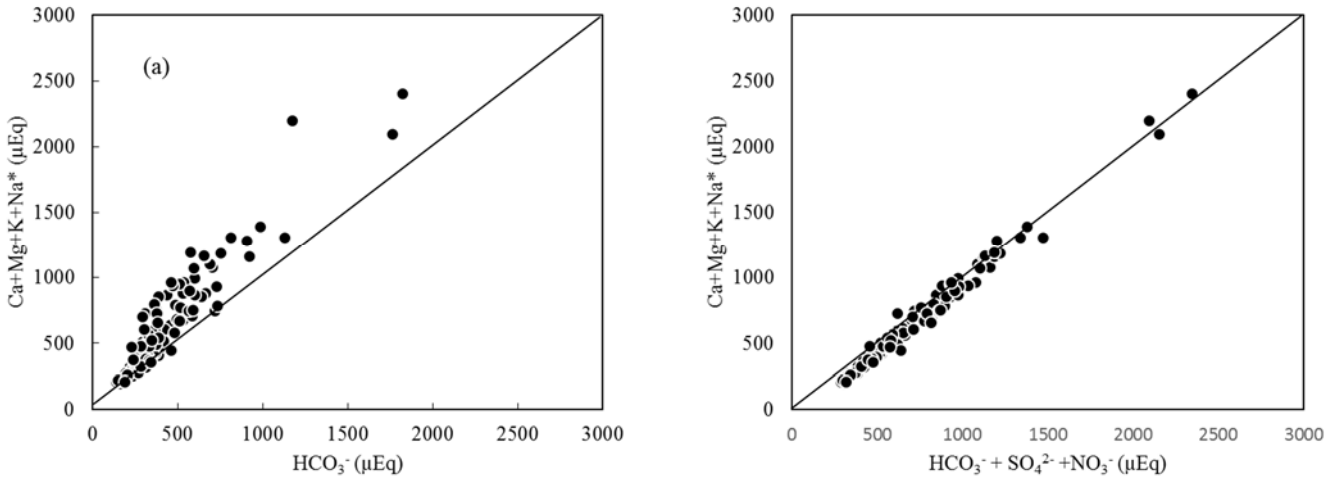

Fig. 6. Plots of total cations derived from carbonate and silicate weathering *vs.* HCO_3^- (a) and $HCO_3^-+SO_4^{2-}+NO_3^-$ (b) for river waters in the SECRB.

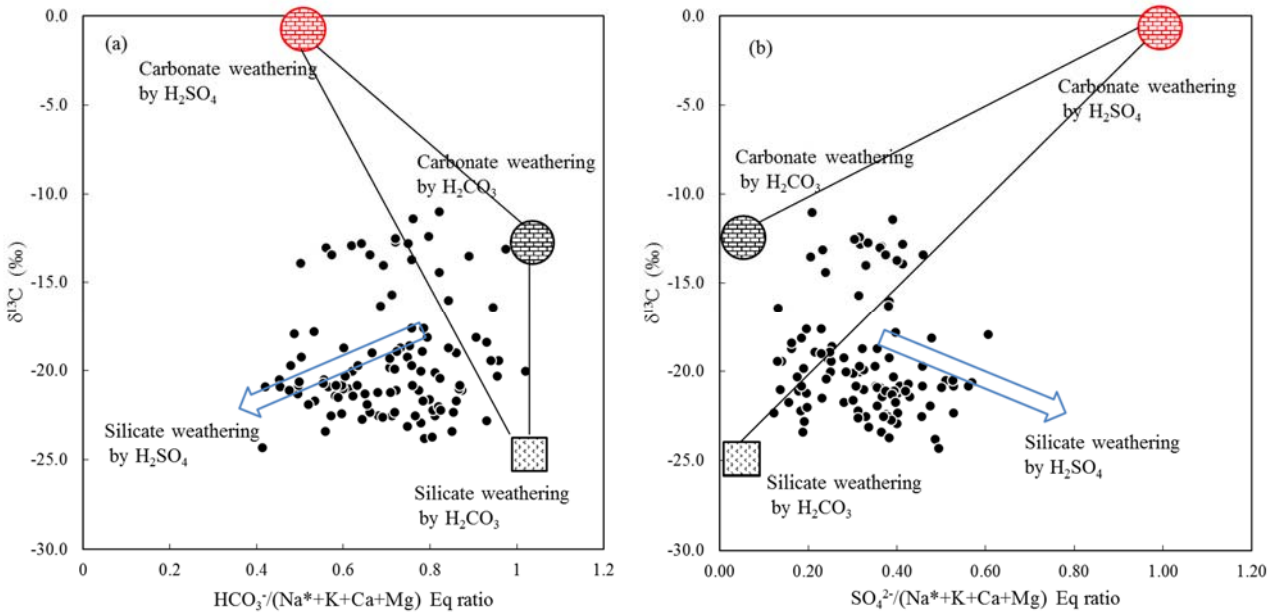

Fig. 7. $\delta^{13}C_{DIC}$ *vs.* $HCO_3^-/(Na^+*+K^++Ca^{2+}+Mg^{2+})$ (a) and $SO_4^{2-}/(Na^+*+K^++Ca^{2+}+Mg^{2+})$ equivalent ratio (b) in river waters draining the SECRB. The plot show that most waters deviate from the three endmember mixing area (carbonate weathering by carbonic acid and sulfuric acid and silicate weathering by carbonic acid), illustrating the effect of sulfuric acid on silicate weathering.